Hedging electricity price spikes with forwards and options*

Simon Brandkamp[†1,2], Peter Cramton[2,3,4], Jason Dark[3], Darrell Hoy[3], and David Malec[3,4]

[1]University of Cologne
[2]Max Planck Institute for Research on Collective Goods, Bonn
[3]Forward Market Design
[4]University of Maryland

2025-02-03

Abstract

Day-ahead electricity markets expose power generators and load-serving entities (LSEs) to large financial risks due to extreme price spikes and correlated load fluctuations. We study how price spikes shape optimal hedging strategies for a risk-averse generator and LSE. Drawing on a regime-switching and dispatch model for ERCOT's day-ahead market, we simulate optimal combinations of forward contracts and call options for granular delivery periods. We find that large and frequent price spikes in a delivery period can result in extreme worst-case losses. Agents, therefore, take larger call option and smaller forwards positions in such spiky periods. Yet combining forwards and options only slightly reduces profit variance and worst-case losses compared to a forwards-only strategy, because profits are almost linear in day-ahead prices. Finally, increasing the option strike price prompts agents to choose larger forwards and smaller options positions. Our findings underscore that hedging with granular derivative products is effective in reducing profit volatility and worst-case losses even when extreme price spikes occur.

*This research is funded by the Deutsche Forschungsgemeinschaft (DFG, German Research Foundation) under Germany's Excellence Strategy – EXC 2126/1-390838866.

[†]E-mail: simon.brandkamp@wiso.uni-koeln.de

1 Introduction

In recent decades, many countries have designed day-ahead electricity markets to procure electricity at the least cost, to integrate fluctuating load and intermittent renewable generation, and to send reliable scarcity signals (Cramton et al., 2017). A downside of day-ahead markets is that they expose market participants to large financial risks. These risks occur because load and day-ahead prices are extremely volatile. Day-ahead electricity prices are far more volatile than prices for most other commodities and assets (Bessembinder and Lemmon (2002), Weron et al. (2004)).[1]

Extreme price spikes partly drive day-ahead price volatility. Between 2011 and 2022, the average day-ahead price was \$43/MWh in the Texas ERCOT market, yet price spikes between \$200/MWh and \$9,000/MWh occurred in almost 900 hours (ERCOT, 2024c). These price spikes arise from price-inelastic electricity demand, the lack of short-term storage, market power, and the strong convexity of the merit order curve (Lu et al., 2005). In the medium term, price volatility and spikes will likely increase further due to growing intermittent renewables and more extreme weather (Ketterer (2014), Peura and Derek W. Bunn (2021)). In the long term, price volatility and spikes might decline if electricity demand becomes more price-elastic or if batteries provide short-term flexibility.

In addition to price risks, market participants face load fluctuations due to changing weather conditions. High load often coincides with day-ahead price spikes (Afanasyev et al., 2015). Because of this positive correlation between load and price spikes, unhedged load-serving entities (LSEs) face large downside risks in day-ahead markets. Unhedged LSEs must procure large quantities at high spike prices, creating a long left tail in their day-ahead profit distribution. For generators, the positive correlation creates an upside opportunity and a right tail in their profit distribution. Hence, the tails in LSE and generators' profit distributions have opposite signs. They require different hedging strategies to hedge their respective right and left profit tails.

This paper simulates optimal hedge strategies for a representative generator and an LSE in ERCOT's day-ahead market. The agents can choose between forward contracts and European call options. Our main research question is how the frequency and size of price spikes in a delivery period affect optimal hedge strategies. Moreover, we study how risk aversion shapes these hedge strategies in the presence of price spikes. We also investigate how the call option's strike price magnitude impacts hedging decisions and profit distributions.

[1]For instance, the standard deviation of the percentage changes in average daily day-ahead prices was 25% in ERCOT between 2011-22. The standard deviation of the daily percentage changes in the S&P 500 stock prices was only 0.93% during the same period. For the WTI oil price, the figure is 2.67%. (Bessembinder and Lemmon, 2002) provide similar statistics for PJM between 1997 and 2000

We begin by simulating the hourly profits of generators and LSEs in ERCOT's day-ahead market between 2011-22. Profits are simulated using the regime-switching model by Coulon et al. (2013), which captures large price spikes. This model simulates joint distributions of hourly day-ahead, gas, and netload prices. We also incorporate solar and wind generation profiles from ERCOT (2023). For each simulated draw of hourly day-ahead price, gas price, and net load, we run a merit order model to obtain hourly dispatch and profits for a sample of 655 power plants in Texas provided by Mann et al. (2017) and ERCOT (2023). We assume that agents' forwards and option positions do not affect bidding behavior or day-ahead prices.

The regime-switching and dispatch models provide realistic distributions of hourly day-ahead profits. Using these distributions, we simulate optimal quantities of forwards and call options for a representative generator and LSE. We define a pair of forward and option quantities as optimal if it maximizes the agent's constant absolute risk aversion utility.

Following Wolak and Hardman (2022) and Cramton et al. (2024), we consider forward and option contracts with granular delivery periods: combinations of year-month-hour-weekend/weekday, such as weekdays 4-5 pm in August 2019. These granular delivery periods allow agents to better manage risks by tailoring hedges to daily and seasonal load or generation cycles (Winzer et al. (2024), Brandkamp (2023)). We assume that agents can buy the granular hedge products at arbitrage-free prices. Ignoring arbitrage opportunities allows us to focus on the risk managing motive for hedging. Our main specification sets a high strike price of \$200/MWh for the call option because the option is intended to primarily cover large price spikes.

We simulate optimal forward and option quantities for all 576 unique granular delivery periods in 2019. We show that the frequency and size of day-ahead price spikes differ sharply across these periods. Spikes tend to be small and rad at night and in winter but larger and more frequent during daytime and summer. These varying levels of "spikiness" allow analyzing how price spikes shape hedge strategies.

Large price spikes can lead to extreme worst-case losses. We find that the LSE and the generators trade-off minimizing worst-case losses versus minimizing profit variance when choosing optimal hedge strategies. They do not optimize expected profit because, with arbitrage-free prices, expected profit is constant no matter how many forwards and options the agent buys. In periods with larger price spikes, the generator and the LSE both rely more on options than forwards to mitigate worst-case losses. The LSE uses options more heavily because price spikes create longer negative profit tails for the LSE than for the generator. Agents' risk aversion is crucial for determining to what extent they focus on worst-case losses or on variance.

Agents who are nearly risk-neutral focus on minimizing profit variance (Min-Var). In low-

spike periods, both sides hold forwards and options in comparable proportions. The LSE typically buys around six times as many forwards as options, while the generator sells five times as many forwards as options. This results in variance-minimizing forward volumes of roughly 90-110% of expected generation for the generator and 100-110% of expected load for the LSE. Min-Var option positions are smaller (about 15-20% of expected quantities for the LSE and 20% for the generator)

In periods with heavier price spikes, the nearly risk-neutral generator only slightly lowers its short-forward ratio and keeps its option ratio constant. By contrast, the nearly risk-neutral LSE strongly reduces its long forward ratio to roughly 80% and increases its option ratio to 30-40%, ending up close to a 2:1 forward-to-option mix. Thus, the LSE heavily relies on options as protection against price spikes even if it is nearly risk-neutral.

The more risk-averse the LSE becomes, the more it shifts focus to ever more extreme parts of its worst-case loss tail. It, therefore, replaces forwards with options, reducing their proportion to almost 2:1 in periods with small spikiness. In spiky periods, the LSE buys even more options than forwards. This strategy reduces tail losses but raises profit variance compared to the Min-Var hedge strategy.

When the generator becomes risk-averse, it reduces its short option position. Shorting options can trigger large losses in spiky delivery periods. For high-risk aversion, the generator, therefore, prefers to buy options than sell them. A long option position offsets the substantial losses from shorting forwards when price spikes occur. The downside is that buying call options increases the variance of the generator's profits because it leads to positive payoffs when the generator's day-ahead profit is high. Therefore, the risk-averse generator increases its short forward position to balance the long option payoff in spiky periods. The generator's long option position is smaller than the LSE's because it has a less extreme worst-case loss tail. The reason is that the generator is more flexible in reducing its generation quantities when prices are unfavorable.

Overall, combining forwards and options is effective in reducing profit variance and worst-case risks compared to a fully unhedged strategy. However, we also compare the combined strategy to a strategy that only hedges with forwards. Surprisingly, the combined strategy only marginally reduces profit variance and achieves only small benefits with respect to worst-case losses compared to the forwards-only strategy. The reason is that the generator and the LSE's day-ahead profits are roughly linear in the day-ahead price. Under linear payoffs, linear forwards hedge effectively, and nonlinear options add little value (Lapan et al., 1991). This explains why nearly risk-neutral agents use few options. The small added benefit of reduced worst-case losses justifies higher option holdings for more risk-averse agents.

Finally, we study how the magnitude of the call option strike price affects hedging in a

delivery period with large price spikes. We analyze strike prices ranging from 100\$/MWh and 1,000\$/MWh. The LSE buys more forwards and fewer options when the strike price rises. With a high strike price, the option offers no protection against moderate spikes, making the option less attractive compared to the forwards. More risk aversion reinforces this tendency, with increased forward buying and decreased option buying. The almost risk-neutral generator also increases its short forwards and decreases its short options when the strike rises. If the generator is risk-averse, long option positions increase in the strike price for low strike prices below 400\$/MWh but decline for higher strike prices.

A low strike price slightly increases agents' profit variance. On the other hand, a low strike price enables the LSE to choose hedge strategies that lead to smaller tail losses, at least when its risk-aversion is low. The reason is that the low strike price induces the LSE to buy more options which leads to lower tail losses but higher variance. In contrast, the higher option holdings chosen under low strike prices increase tail losses for the generator unless it is very risk averse.

It therefore depends on agent's risk preferences which strike price the market designer should choose. A smaller strike price has the advantage that it offers better spike protection for the LSE. The LSE has less flexibility and is more vulnerable to extreme negative profit tails than the generator. Some researchers also opt for low strike prices because low strikes might improve generators' strategic bidding incentives in day-ahead markets (Willems (2005), Zhang et al., 2012). Yet, determining the exact strike price level requires further research.

Our paper shows that forwards and options enable participants in day-ahead markets to effectively manage risk in extreme price spikes. Regulators should encourage hedging by establishing liquid markets for forwards and options with standardized contracts. Obliging LSEs to hedge a certain share of their expected load could also increase liquidity and coordinate trade (Cramton et al., 2024).

High liquidity will mitigate price premia and arbitrage between day-ahead and derivative markets. Regulators could further reduce price premia by facilitating arbitrageurs and financial institutions to trade in electricity markets. However, some level of price premia will likely persist even in liquid electricity markets. It would be interesting to study how the above optimal hedging strategies change when arbitrage is possible. Finally, future research could study in which market equilibria the generator and LSE's strategies result.

The following section relates our paper to the literature on optimal hedging strategies in electricity markets. Section 3 introduces the generator and LSE's profit and utility functions. Section 4 describes the simulation of the day-ahead market profits, including the regime-switching model and the merit order dispatch model. Section 5 defines the forwards and option contracts and calculates arbitrage-free forwards and option prices.

Section 6 simulates optimal hedging strategies and examines how they depend on price spikes and risk preferences. Section 7 concludes.

2 Literature review

Hedging is essential in day-ahead markets for electricity generators and load-serving entities (LSEs). their load and day-ahead prices fluctuate strongly, creating extreme financial risks.

Forward contracts are the most widely used hedging instrument for generators and LSEs (S.-J. Deng and Oren, 2006). A comprehensive literature identifies the optimal forward quantity a commodity producer or consumer should buy. Danthine (1978), Holthausen (1979), Feder et al. (1980), and McKinnon (1967) show that when price and quantity uncertainties are independent, agents should sell exactly their expected quantity forward. They can sell less than their expected quantity forward if they are flexible to change their quantity in response to fluctuating prices, as most electricity generators are (Moschini and Lapan (1992), Dionne and Santugini (2015)). McKinnon (1967), Rolfo (1980), Losq (1982), Lapan and Moschini (1994), and Borenstein (2007) reveal that agents hedge more than their expected quantity when prices and output are positively correlated. LSEs often face such a positive correlation. Jin (2007) and Lien (2010) show that a right-skewed profit distribution also increases the optimal forward position for producers. Building on the above theoretical insights, many studies identify the optimal quantity of forward contracts for electricity generators (Näsäkkälä and Keppo (2005), Conejo et al. (2008)) and load-serving entities (Woo et al. (2004), Kettunen et al. (2009), T. Deng et al. (2020)). Yet, several researchers argue that linear forward contracts alone are an ineffective hedging instrument if day-ahead market profits are not linear in the day-ahead price. Nonlinearity arises if load and prices are correlated (Sakong et al., 1993), if load or generation is price-elastic (Moschini and Lapan, 1992), or if cost functions are nonlinear.

Various papers demonstrate that nonlinear profits can be hedged effectively by combining linear forwards with nonlinear derivatives such as options (Moschini and Lapan (1992), Moschini and Lapan (1995), Oum et al. (2006)). Oum and Oren (2010), Zhou et al. (2017), and Hess (2021) describe the optimal combination of forwards and options for LSEs. They emphasize that hedging with options is beneficial for LSEs since they face large non-traded uncertainty in the load that is correlated with prices. Oum et al. (2006) and Oum and Oren (2010) obtain the optimal payoff function of an exotic option for an LSE and show that this optimal payoff function can be replicated with a portfolio of forwards and standard European options. For generators, Azevedo et al. (2007), Sanchez et al. (2010) and Ocakoglu and Tolga A. (2018) also stress the benefits of combining

options and forwards. Other authors emphasize the advantages of combining electricity forward contracts with exotic swing or Asian options (Hambly et al. (2008), Fanelli et al. (2016)), fuel-spread options (Aïd et al. (2013)), or weather derivatives (Lee and Oren (2009), Bhattacharya et al. (2020), Matsumoto and Yamada (2021)).

While options and forwards are useful risk-management tools, agents can also use them to speculate if forward and option prices are not arbitrage-free. Forwards and options can skew the profit distribution to the right if arbitrage opportunities exist (Lapan et al. (1991), Vercammen (1995)). Lien (2010) show that price spikes increase the optimal forward position of producers when the forward price is larger than the expected day-ahead price and reduce the forward position when the forward price is negatively biased. Arbitrage opportunities between day-ahead, and forward and option markets are widespread in electricity markets and are an important driver of hedging behavior (Redl et al. (2009), Botterud et al. (2010)). Nevertheless, in this paper, we focus on arbitrage-free prices to study the risk management motive for hedging in isolation.

Large day-ahead price spikes are another important factor that shapes LSE and generators' hedge strategies. Price spikes make generators' day-ahead profit distribution right-skewed and LSEs distribution left-skewed. Vercammen (1995) and Barbi and Romagnoli (2018) point out that agents can use forwards and options to reshape their profit distributions. LSEs can go long in forwards and options to offset their negative tail and thereby reduce worst-case losses. For generators, spike prices lead to large upside potential that is reduced by short positions. Vercammen (1995) shows that risk-averse generators might still prefer short forward and option positions to lower profit volatility, but short positions can cause large worst-case losses if price spikes occur. Bessembinder and Lemmon (2002) suggest that such spikes create a risk premium in forward and option prices since risk-averse generators and speculators require compensation for short positions. LSEs, meanwhile, should be willing to pay this premium to avoid large losses under spike conditions.

Traditionally, researchers model price spikes by assuming lognormally distributed day-ahead prices, enabling closed-form solutions for forward and option positions under mean-variance or CARA utility (Oum et al., 2006). In recent years, however, price spikes have become so extreme that lognormal distributions no longer fit. Numerous authors instead use regime-switching models to describe these extreme price spikes (Hamilton (1990), de Jong and Huisman (2002), Weron et al. (2004)). Coulon et al. (2013) simulate quantities for forwards and options, respectively, that separately minimize profit variance for an LSE. They also provide suggestive evidence that combining options and forwards will further reduce profit variance. Yet, LSEs and generators may also worry about downside tail risks if prices spike severely, so they might not minimize variance alone. Risk-averse LSEs with large negative profit tails could prioritize worst-case losses over mere variance

reduction.

We therefore extend Coulon et al.'s (2013) in three ways. First, we derive combined optimal forward and option positions for LSEs and generators under extreme price spikes, assuming CARA utility. We study how the level of risk aversion influences hedging strategies and profit distributions. Supplementing Coulon et al.'s (2013) analysis, we also compare a combined forward–option strategy to a forward-only strategy.

Second, we examine how option and forward quantities change with the "spikiness" of a given delivery period's price distribution, measured via the option-to-forward price ratio, which is strongly correlated with spike size and frequency.

Third, we investigate how the call option's strike price influences hedging effectiveness in high-spike conditions. This analysis builds on Oum et al. (2006), and shows how forward and option quantities depend on the option's strike prices. We study how the strike price affects profit variance and tail profits.

3 Hedging with forwards and options

This section describes how electricity generators and load-serving entities (LSE) determine the optimal quantities of forwards and call option contracts. LSE and generator's (GEN) respective profits from selling electricity in the day-ahead market in hourly period t are

$$\pi_{DA_t}^{LSE} = (R_Y - P_t)q_t \qquad \pi_{DA_t}^{GEN} = P_t q_t - c_t(q_t)$$

P_t denotes the day-ahead electricity price in hour t. q_t is the load that the LSE procures or the generator produces. R_Y is the fixed retail price in year Y that the LSE charges to its end-consumers. $c_t(q_t)$ represents the generator's cost function. The shape of $c_t(q_t)$ changes over time since generation costs change with fuel prices.

Generators and LSEs can hedge their day-ahead market risk by purchasing forwards or call option contracts. The focus on forwards and call options is not restrictive because the combination of these contracts can replicate positions equal to many other classical derivatives, including put and straddle positions (Cox and Rubinstein, 1985). When buying forwards and call options, agent $i \in \{\text{LSE, GEN}\}$ has the following profit function in each hourly period $t \in M$:

$$\pi_t^i = \pi_{DA_t}^i - (F_M^p - P_t)h_M - (V_M - v_t)z_M$$

h_M is the quantity of forward contract M agent i buys. M defines the delivery period that the forward and option contracts cover. For instance, M could contain all baseload

hours in June 2026. If $h_M = 1MW$, this means that the agent would buy $1MW$ of forward energy in all baseload hours in June 2026 (Coulon et al., 2013). F_M^p is the forward price for contract M. V_M is the price for the call option, z_M is the quantity of option contracts, and v_t is the gross value of the call option defined as:

$$v_t = \begin{cases} P_t - K_M & \text{if } P_t \geq K_M \\ 0 & \text{if } P_t < K_M \end{cases}$$

K_M is the option's strike price. Forward and option quantities h_M and z_M can be positive or negative. A negative quantity means that agent i sells electricity forward or sells a call option. It might seem natural that LSEs want to buy electricity forward and generators want to sell it. However, LSEs and generators can buy positive and negative quantities. Importantly, we assume that the chosen forwards and option prices do not affect prices and quantities in the day-ahead markets. Several authors reveal that forward and option positions improve bidding incentives and make day-ahead market equilibria more competitive (Allaz and Vila (1993), Willems (2005), Zhang et al. (2012)). We abstract from these effects in our day-ahead market simulation.

When agent i chooses the optimal quantities of forwards h_M and options z_M, she faces uncertainty about the day-ahead price P_t and her realized load q_t in period t. The generator's cost function $c_t(q_t)$ is also uncertain when forward and option quantities are chosen because $c_t(q_t)$ depends on fuel prices in period t. Given this uncertainty, agent i chooses the optimal z_M and h_M for contract M that maximize its expected utility:

$$\underset{h_M, z_M}{max}\ E[U(\pi^i_{t \in M})]$$

The first-order conditions are given as:

$$\frac{\partial E[U(\pi^i_t)]}{\partial H} = E[U\prime(\pi^i_{t \in M})(F^p_M - P_{t \in M})] = 0$$
$$\frac{\partial E[U(\pi^i_t)]}{\partial Z} = E[U\prime(\pi^i_{t\ inM})((v_{t \in M} - V_M))] = 0$$

If we aimed to solve this problem analytically, we would have to make assumptions about the shape of the utility function and the joint distribution of the random factors prices, load, and costs (Moschini and Lapan, 1995). Several authors solve variants of this problem analytically, assuming a constant absolute risk aversion (CARA) utility function and joint normally distributed load and prices (Lapan et al. (1991), Moschini and Lapan (1995)). We will not follow their approach because load and prices are not jointly normally distributed for electricity generators and LSEs. The main reason is that the electricity price distribution is strongly right-skewed. Assuming a normal distribution of electricity

prices is not suitable for us, since we are interested in how to hedge when prices exhibit large spikes. Hence, we will assume a CARA utility function and solve the above problem numerically. To do so, the next section describes a regime-switching model of the ERCOT day-ahead market that allows simulating strongly skewed distributions of prices, load, and costs.

4 Day-ahead market simulation

4.1 Regime-switching model

This section aims to simulate realistic distributions of generators and LSEs' day-ahead market profits. In section 4.1, we follow Coulon et al. (2013) and build a regime-switching model that allows estimating the joint distribution of the most relevant determinants of day-ahead profits: day-ahead prices, gas prices, net load, and solar and wind generation. To calibrate the model, we use data on hourly day-ahead prices from ERCOT (2024c), and hourly system load data from ERCOT (2024b) for all hours from 2011 to 2022. Moreover, we use daily Henry Hub gas price data for 2011-22 from (EIA,2024). We also use hourly generation profiles for 218 wind farms and 189 solar farms that actually operate in ERCOT. The generation profiles were created by ERCOT (2023). In addition, we use data on hourly solar and wind generation from ERCOT (2024a).

Figure 1a depicts the average daily day-ahead electricity price in ERCOT and the daily Henry Hub gas price between 2011 and 2022. Modeling the day-ahead electricity prices is challenging because they experience extreme spikes. Moreover, day-ahead prices follow strong seasonal, weekly, and daily cycles.

The literature that aims to model these features can be broadly categorized into two streams. The first stream consists of structural models. These models derive electricity prices from a merit order approach that considers the costs of all power plants and their operational constraints. An advantage of a structural model is that it offers an intuitive explanation of price formation and allows analyzing how capacity expansion and changes in the resource structure affect electricity prices (Carmona et al., 2013). A disadvantage is that structural models struggle to explain extreme price spikes where prices far exceed generators' marginal costs. The second literature stream uses reduced-form models. Such models describe the evolution of electricity prices as a pre-specified stochastic process. They often include price spikes using regime-switching or jump processes. However, reduced models do not capture how price spikes depend on the factors that influence electricity prices, like fuel prices, outages, and load (Carmona et al., 2013). Most importantly for our purpose of deriving optimal hedge positions, a model of day-ahead profits must

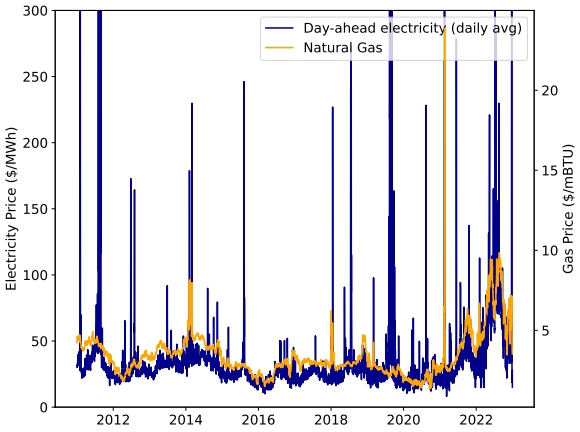

(a) Daily Average Electricity and Gas Prices (Electricity Prices Capped at $300/MWh)

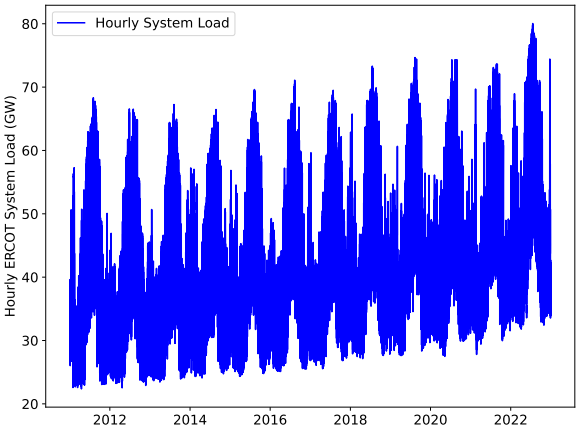

(b) Hourly ERCOT System Load

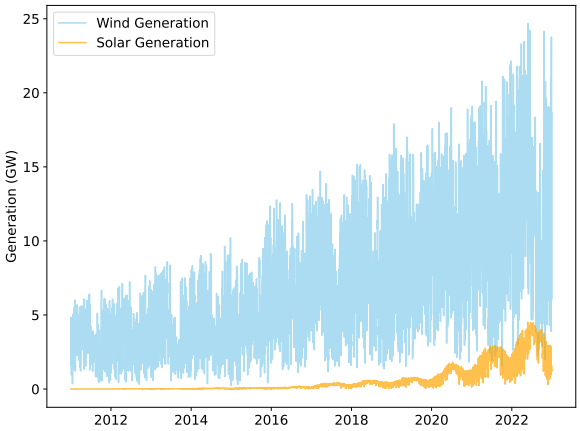

(c) Daily Average Aggregate Wind and Solar Generation in ERCOT

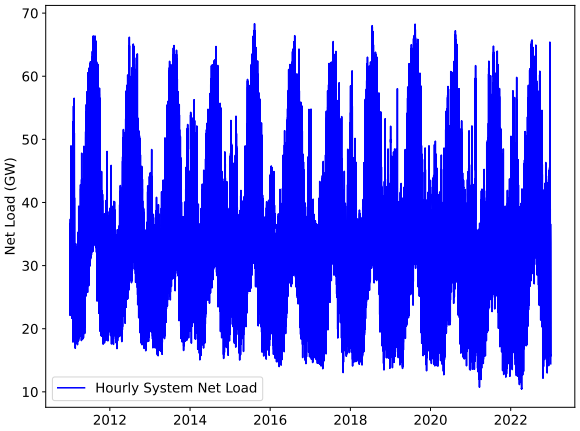

(d) Hourly ERCOT System Net Load

Figure 1: Empirical data from ERCOT on prices, renewable generation, and load in 2011-22

capture that price spikes are positively correlated with load and gas prices.

Following Barlow (2002), several authors combined the two above literature streams. They describe electricity day-ahead prices as a function of relevant determinants, especially load and fuel prices. These determinants are assumed to follow correlated stochastic processes. In some models, the determinants influence the probability of a price jump or regime switch to account for price spikes. Most models include load (Barlow, 2002) and fuel prices (Carmona et al., 2013) as crucial determinants of power prices. The literature considers gas as a marginal fuel to explain most variation in electricity prices (Füss et al., 2015). In Carmona et al.' 2013, the electricity price depends on multiple fuels like coal and gas. Other authors also include plant outages as a determinant for power prices.

This paper employs such a combined regime-switching model by Coulon et al. (2013). In their model, the following equation describes the hourly day-ahead electricity price P_t:

$$P_t = G_t \exp\left(\alpha_{m_k} + \beta_{m_k} L_t + \gamma_{m_k} X_t\right) \tag{1}$$

G_t is the daily gas price, and L_t is the hourly net load, i.e., load minus intermittent solar and wind generation. X_t is a residual process and $m_k \in \{1, 2\}$ indicates whether prices are in the normal price regime 1 or in the spike price regime 2. The above exponential expression for the electricity spot price is commonly used in the literature (Eydeland and Geman, 1999). The advantage of this exponential form is that the resulting day-ahead prices P_t are lognormally distributed in each price regime. This allows for deriving closed-form solutions for forward and option prices (Coulon et al. (2013), Füss et al. (2015)).

Following Coulon et al. (2013), we rely on gas as the price-setting marginal fuel. Figure 1a reveals that average daily electricity prices are closely linked to daily gas prices, even though daily electricity prices show larger spikes than gas prices. We model logarithmic gas prices G_t as an Ornstein-Uhlenbeck (OU) process (Coulon et al. (2013), Schwartz (1997)).

$$d\log G_t = \kappa_G(m_G - \log G_t)dt + \eta_G dW_t^{(G)} \tag{2}$$

In contrast to Coulon et al. (2013), we use net load L_t rather than load as a second determinant of power prices in equation 1. Coulon et al. (2013) use load because solar and wind generation was still negligible in Texas during their observation period between 2005 and 2011. Over the last decade, the rising share of wind and solar generation has become an important determinant of day-ahead electricity prices. Solar and wind plants have near-zero marginal costs and are usually dispatched when there is sun or wind and no curtailment. Since intermittent renewable generation shifts the merit order curve, netload rather than load determines prices in day-ahead markets with significant renewable generation (Ketterer (2014), Peura and Derek W. Bunn (2021)).

Figure 1b reveals that ERCOT's hourly system load shows strong predictable seasonal cycles and is increasing over time. Figure 1c highlights that the aggregate solar and wind generation is also increasing over time. Surprisingly, Figure 1d indicates that hourly net load is not increasing even though load and solar and wind generation are all increasing. Even the daily standard deviation of the netload stays relatively stable over time. This suggests a strong positive correlation between load and solar and wind generation in ERCOT.

Following Coulon et al. (2013), we decompose net load L_t into a seasonal component $S(t)$ and a deseasonalized component $\overline{L}_t$.

$$L_t = S(t) + \overline{L}_t \tag{3}$$

Seasonal component $S(t)$ is estimated separately for every hour h of the day.

$$S(t) = a_1(h) + a_2(h)\cos(2\pi t + a_3(h)) + a_4(h)\cos(4\pi t + a_5(h)) + a_6(h)t + a_7(h)1_{we} \tag{4}$$

a_1 represents the long-term average net load in hour h. a_2 controls the amplitude of seasonal variations while a_3 sets the starting point of the seasonal cycles. Similarly, a_4 and a_5 capture higher-frequency daily net load cycles. a_6 describes long-term linear trends, and a_7 considers that net load is typically lower on weekends. Deseasonalized net load $\overline{L}_t$ is modeled by the following OU process:

$$d\bar{L}_t = -\kappa_L \bar{L}_t\, dt + \eta_L\, dW_t^{(L)} \tag{5}$$

The above process models deseasonalized net load to be normally distributed and mean-reverting. The deseasonalized net load process and the gas price process in equation 2 are assumed to be uncorrelated (i.e., $W_t^{(L)}$ and $W_t^{(G)}$ are independent).

While net load and gas prices are crucial, there are additional important determinants of power prices, such as generator or transmission outages. Coulon et al. (2013) do not explicitly model these factors but include them as a residual, unobserved process X_t.

$$X_t = S_X(t) + \bar{X}_t \tag{6}$$

$S_X(t)$ is the seasonal component of X_t that accounts for seasonal and daily cycles in the frequency of outages and transmission constraints.

$$S_X(t) = b_1(h) + b_2(h)\cos(2\pi t + b_3(h)) + b_4(h)\cos(4\pi t + b_5(h)) \tag{7}$$

As above, the deseasonalized residual $\bar{X}_t$ follows an OU process

$$d\bar{X}_t = -\kappa_X \bar{X}_t \, dt + \eta_X \, dW_t^{(X)} \tag{8}$$

The random elements of the deseasonalized net load $W_t^{(L)}$ and the desaeasonalized residual load $W_t^{(X)}$ are allowed to be correlated. Transmission or generator outages are more likely under extreme weather conditions when net load is typically high. $\bar{L}_t$ and $\bar{X}_t$ are OU processes with mean zero since their means are substracted by their seasonal components $S(t)$ and $S_X(t)$.

In day-ahead price equation 1, indicator m_k determines whether prices are in normal regime 1 or spike regime 2. m_k is chosen by an independent coin flip:

$$m_k = \begin{cases} 1 & \text{with probability } 1 - p_s \Phi\left(\frac{\bar{L}_t - \mu_s}{\sigma_s}\right) \\ 2 & \text{with probability } p_s \Phi\left(\frac{\bar{L}_t - \mu_s}{\sigma_s}\right) \end{cases}$$

The probability of being in spike regime 2 increases in deseasonalized net load $\overline{L}_t$. $\phi(\cdot)$ is the normal cumulative distribution function (cdf). p_s gives the probability of being in spike regime 2 when $\overline{L}_t$ goes to infinity. μ_s and σ_s are parameters that govern how the spike probability depends on deseasonalized net load. Following Coulon et al. (2013), we set $\mu_s = 0$ and $\sigma_s = \frac{\eta_L}{\sqrt{2\kappa_L}}$ such that the parameters equal the mean and standard deviation of the stationary distribution of observed deseasonalized net load $\bar{L}_t$. Thereby, the probability of a price spike becomes linear in the quantile of $\bar{L}_t$ (Coulon et al., 2013).

Day-ahead price equation 1 has the same exponential form for regimes 1 and 2. Since the parameters α_{m_k}, β_{m_k}, and γ_{m_k} differ between the two regimes, the model allows for a steeper relationship between net load and prices in spike regime 2 (Coulon et al., 2013).

4.2 Simulating day-ahead market outcomes

In this section, we simulate hourly day-ahead market states, i.e., we draw values from the joint distribution of day-ahead electricity prices, gas prices, net load, and solar and wind generation.

We first estimate the parameters of the day-ahead price equation 1 using data on hourly day-ahead electricity prices, net load, and daily gas prices between 2011 and 2022. To do so, we fit the seasonal net load component coefficients $S(t)$ in equation 4. The estimated coefficients can be found in Table 4 in appendix A for every hour of the day. Figure 2 shows net load and its seasonal components for weekends and weekdays for 8 am and 4 pm.[2] The figure reveals that seasonal variation in net load is much larger for the peak hour

[2]Figure 2 was also created by Coulon et al. (2013) and is replicated here for our different observation

4 pm compared to the less peaky hour 8 am. After calculating the seasonal component of net load, we obtain the deseasonalized net load $\overline{L}_t$ using equation 3.

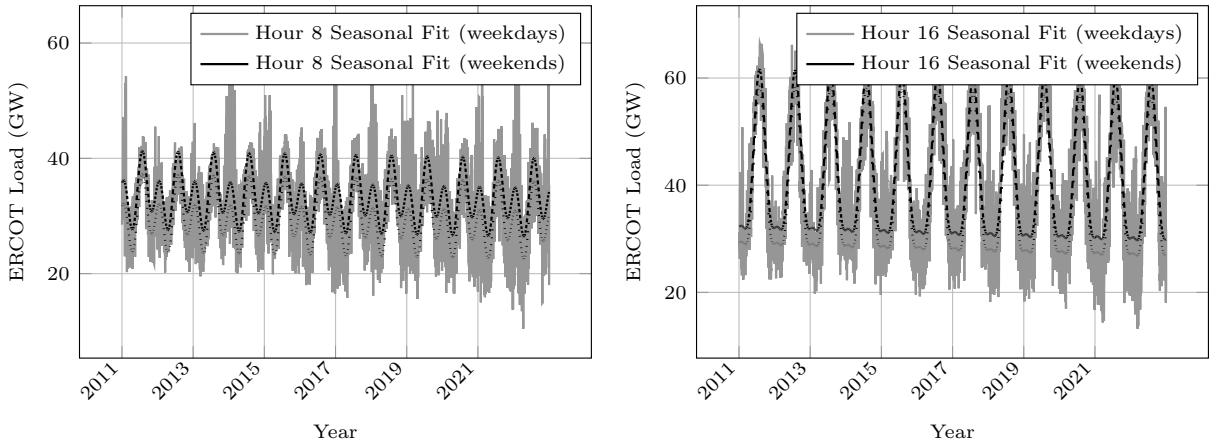

(a) Hour 8 Seasonal Component

(b) Hour 16 Seasonal Component

Figure 2: ERCOT System Load Seasonal Components for Hours 8 and 16.

We can now estimate the remaining parameters in price equation 1 using the likelihood function[3]

$$\mathcal{L}^P(\alpha_1,\alpha_2,\beta_1,\beta_2,\gamma_1,\gamma_2,p_2) = \prod_t \left\{ p_s \phi\left(\frac{\overline{L}_t-\mu_s}{\sigma_s}\right) \frac{1}{\gamma_2\sqrt{2\pi}} \exp\left(-\left(\frac{\log\left(\frac{P_t}{G_t}\right)-\alpha_2-\beta_2 L_t}{\gamma_2}\right)^2\right) \right. \tag{9}$$
$$\left. + \left(1-p_s\phi\left(\frac{\overline{L}_t-\mu_s}{\sigma_s}\right)\right) \frac{1}{\gamma_1\sqrt{2\pi}} \exp\left(-\left(\frac{\log\left(\frac{P_t}{G_t}\right)-\alpha_1-\beta_1 L_t}{\gamma_1}\right)^2\right) \right\}$$

The estimation models the deseasonalized residual process X_t as normal random noise (Coulon et al., 2013). The estimated parameters are given in Table 1.

α_1	β_1	γ_1	α_2	β_2	γ_2	p_s
1.279	2.39×10^{-5}	0.308	-0.035	7.12×10^{-5}	1.065	0.161

Table 1: Estimated parameters for the day-ahead price function in equation 1

As expected, $\beta_2 > \beta_1$ which means that the exponential relation between net load and prices is steeper in spike price regime 2 than in price regime 1. $\gamma_2 > \gamma_1$ implies that random shocks like plant outages also have a stronger effect on prices in the spike regime than in the normal regime. $p_s = 16.1\%$ reveals that prices are in the spike regime in $8.05\%(p_s/2)$ period.

[3]We follow Coulon et al. (2013) and remove all hourly observations where $P_t/G_t < 0.1$, i.e., the electricity price is very small relative to the gas price. Only 6 out of 105,158 hours are removed. Eliminating these small outliers is supposed to improve the fit of the likelihood estimation (Coulon et al., 2013).

of hours because the spike probability $p_s\Phi\left(\frac{\bar{L}_t-\mu_s}{\sigma_s}\right)$ fluctuates symmetrically between 0 and p_s in each hour t (Coulon et al., 2013).

Using the estimated parameters in Table 1, we rearrange price equation 1 to back out the residual process X_t.

$$X_t = p_s\phi\left(\frac{\overline{L}_t-\mu_s}{\sigma_s}\right)\left(\frac{\log\left(\frac{P_t}{G_t}\right)-\alpha_2-\beta_2 L_t}{\gamma_2}\right)+\left(1-p_s\phi\left(\frac{\overline{L}_t-\mu_s}{\sigma_s}\right)\right)\left(\frac{\log\left(\frac{P_t}{G_t}\right)-\alpha_1-\beta_1 L_t}{\gamma_1}\right)$$

Afterward we employ equation 7 to fit the seasonal component $S_X(t)$ (see Table 4 in appendix A for the estimated coefficients) and obtain the deseasonalized residual process $\overline{X}_t$ using equation 6. Having determined $\overline{L}_t$ and $\overline{X}_t$, we now jointly estimate the parameters of the correlated OU processes $d\bar{L}_t$ and $d\bar{X}_t$ in equations 5 and 8 by maximizing the following likelihood function

$$\mathcal{L}^{OU}(\kappa_L,\eta_L,\kappa_X,\eta_X,\nu)=\prod_{t=2}^{N}\frac{1}{2\pi\sqrt{\det(\Sigma)}}\exp\left(-\frac{1}{2}\mathbf{I_t}^T\Sigma^{-1}\mathbf{I_t}\right)$$

with $\mathbf{I_t}=\begin{pmatrix}d\bar{L}_t\\ d\bar{X}_t\end{pmatrix}$. The variance-covariance matrix of the bivariate normal processes is

$$\Sigma=\begin{pmatrix}\sigma_L^2 & \nu\sigma_L\sigma_X\\ \nu\sigma_L\sigma_X & \sigma_X^2\end{pmatrix} \tag{10}$$

ν is the correlation coefficient between $d\bar{L}_t$ and $\bar{X}_t$, $\sigma_L^2=\frac{\eta_L^2(1-e^{-2\kappa_L dt})}{2\kappa_L}$ is the variance of $d\bar{L}_t$, and $\sigma_X^2=\frac{\eta_X^2(1-e^{-2\kappa_X dt})}{2\kappa_X}$ is the variance of $\bar{X}_t$.

Similarly, we maximize the following likelihood function to estimate the parameters of the OU process of the log gas price, assuming that $d\log G_t$ is not correlated with $d\bar{L}_t$ and $d\bar{X}_t$.

$$\mathcal{L}^{G}(\kappa_G,m_G,eta_G)=\frac{1}{\sqrt{2\pi\eta_G^2 dt}}\exp\left(-\frac{(d\log G_t-\kappa_G(m_G-\log G_t)dt)^2}{2\eta_G^2 dt}\right)$$

The estimated parameters for the three OU processes are shown in Table 2.

κ_L	η_L	κ_G	η_G	m_G	κ_X	η_X	ν
125.571	84,329.524	3.524	0.915	1.159	996.966	40.406	0.092

Table 2: Parameters relating to the stochastic processes for G_t, L_t, and X_t.

$\kappa_G = 3.524$ reveals that gas prices need more than two months to revert to their mean.

However, gas prices mean-revert much faster from 2011-22 than from 2005-11 as estimated by Coulon et al. (2013). $\kappa_L = 125.571$ indicates that the net load typically requires around two days to revert to its seasonal mean, reflecting the net load's dependence on multi-day weather movements. Netload mean-reverts slightly slower than load in Coulon et al.'s (2013) earlier time period because the net load is likely more weather dependent than load. Deseasonalized net load is volatile as the large η_L indicates. $\kappa_X = 996.966$ implies that the residual process reverts to its seasonal mean after roughly 6 hours. Plant or transmission outages likely only affect prices for a couple of hours, as Coulon et al. (2013) also find.

Using the above estimated parameters we simulate the deseasonalized OU processes for the load, log gas prices, and the residual process. After adding their seasonal components, we insert the simulated values for net load, gas price and the residual process into equation 1 to calculate the corresponding day-ahead electricity prices.

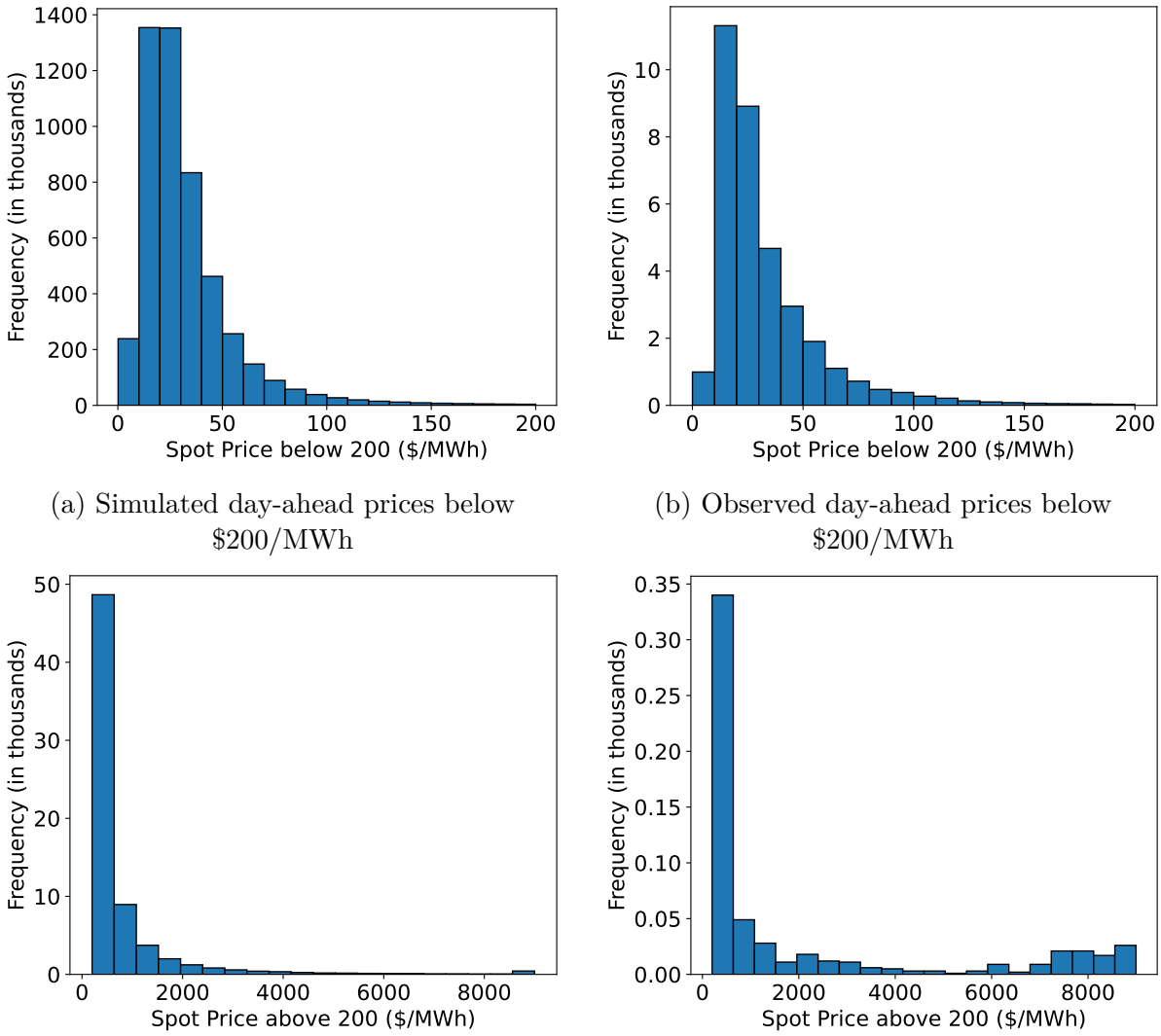

(a) Simulated day-ahead prices below $200/MWh

(b) Observed day-ahead prices below $200/MWh

(c) Simulated day-ahead prices above $200/MWh

(d) Observed day-ahead prices above $200/MWh

Figure 3: Histogram of day-ahead electricity prices below and above $200/MWh for simulated and observed data between 2019-22

To examine how well the simulated prices and quantities match the observed empirical values, we simulate 20 market states for each of the 105,158 observed hourly periods, leaving us with more than 2.1 million simulated market states. Figure 3 compares the histograms of the simulated hourly day-ahead prices (left side) with the histograms of the day-ahead prices that were observed in ERCOT between 2011-22 (right side). Figures 3a and 3b show the distribution of the simulated and observed "normal" prices below $200/MWh. The simulated and observed distributions below $200/MWh look similar and resemble a lognormal distribution. The standard deviation of the simulated prices below $200/MWh is $23.1/MWh, slightly smaller than the standard deviation of $25.0/MWh for the observed prices.

Figures 3c and 3d depict the distribution of price spikes above \$200/MWh. 1.4% of the simulated prices and 1.7% of the observed prices exceed \$200/MWh. In rare cases, the regime-switching model simulates unreasonably large day-ahead prices since the model does not consider the administrative price cap of \$9,000/MWh. In only 0.007% of the simulated hours, prices exceed the cap of \$9,000/MWh. To make the simulated prices consistent with the actually observed prices, we also cap prices at \$9,000/MWh. Simulated spike prices are mostly smaller than \$4,000/MWh. In contrast, a larger share of observed spike prices falls between \$4,000/MWh and \$9,000/MWh. This shows that there is room for improving our simulation of the long right-tail of day-ahead prices. However, we believe that our model captures price spikes in ERCOT reasonably well to analyze the effects of the price spikes on hedging behavior.

In Appendix C, we also compare the simulated and observed distributions for gas prices, net load, and load. To derive load, we also simulate aggregate wind and solar generation using wind and solar generation profiles provided by ERCOT (2023). The wind and solar generation model is also presented in appendix B.

4.3 Day-ahead market quantities and profits

We calculate generators and LSE's load in every market state based on the above day-ahead market states. For LSEs, load is assumed to be price-inelastic and to be related to aggregate load Q_t as follows:

$$q_t = sQ_t + \varepsilon_t$$

s is a fixed market share of the LSE. ε_t is a random noise process such that the LSE's load fluctuates around its share in aggregate load (Peura and Derek W. Bunn, 2021).

To determine generation quantities and profits for power plants, we employ the merit order dispatch model proposed by Mann et al. (2017). We compiled a dataset of 655 power plants located in Texas. Table 3 shows the number of power plants and their nameplate capacity by generation technology. Except for wind and solar plants, data on capacity, commissioning dates, heat rates, and variable costs are borrowed from Mann et al. (2017). For solar and wind farms, data on capacity and commissioning dates are obtained from ERCOT (2023) and are supplemented by web searches for some individual plants. Marginal costs for power plant GEN are (Mann et al., 2017).

$$c_t^{GEN} = FP_t^{GEN} * \text{Marginal heat rate}^{GEN} + \text{Variable O\&M Cost}^{GEN}$$

c_t^{GEN} is zero for solar, wind, hydro, and biomass plants (Mann et al., 2017). For all other technologies, marginal costs fluctuate with their fuel price FP_t^{GEN}. Fuel prices

Technology	Plant Count	Capacity (MW)	% in Total Capacity
Wind	218	39,203	27.29
Solar	189	24,701	17.19
Gas Combined Cycle	68	35,132	24.45
Gas Steam Turbine	46	11,970	8.33
Gas Open Cycle	83	6,438	4.48
Gas Combustion Engine	10	671	0.47
Lignite	12	7,142	4.97
Coal	20	12,637	8.80
Hydro	5	555	0.39
Nuclear	4	4,981	3.47
Biogas	4	93	0.06
Biomass	2	150	0.10

Table 3: Overview of plant types, their counts, nameplate capacities, and shares in total capacity.

for biomass and uranium are taken from Mann et al. (2017) and are held constant over time. Prices for coal and lignite in Texas are assumed to change on a yearly basis and are provided by (EIA, 2028) and (EIA,2023). We allow the gas price to change on a daily basis following the Henry hub wholesale market gas price (EIA,2024). Figure 1a in section 4.1 plots the daily gas price during our simulation period. We ignore fixed costs for all generation technologies. In every period, each plant has a forced outage with a probability of 15%

For the merit order model, we first focus on dispatchable power plants (all plants except wind and solar). Let $N_t = 1, 2, ..., n$ be the list of dispatchable power plants that do not have an outage in period t. Plants in N_t are sorted by their marginal costs such that $c_t^1 \leq c_t^2 ... \leq c_t^n$. Each plant's marginal cost and its position in the merit order list N_t varies over time according to its time-varying fuel price FP_t^{GEN}. In every period t, the goal of the merit order dispatch model is to choose each plant's generation q_t^i such that the aggregate costs of electricity generation are minimized.

$$\min_{\{q_t^i\}} \sum_{i=1}^{n} c_t^i q_t^i$$

subject to the constraints that the aggregate generation of dispatchable plants equals aggregate net load and that each plant respects its capacity limits.

$$\sum_{i=1}^{n} q_t^i = L_t$$
$$0 \leq q_t^i \leq q_{\max}^i, \quad \forall i \in N$$

To meet these constraints and achieve the cost-minimizing dispatch, we start with the

first plant in the merit order and dispatch each plant at its maximum capacity until the cumulative dispatched capacity meets or exceeds the netload.

$$q_t^i = \begin{cases} q_{\max}^i, & \text{if } \sum_{j=1}^{i} q_{\max}^j \leq L_t \\ L_t - \sum_{j=1}^{i-1} q_{\max}^j, & \text{if } \sum_{j=1}^{i-1} q_{\max}^j < L_t \leq \sum_{j=1}^{i} q_{\max}^j \\ 0, & \text{if } \sum_{j=1}^{i-1} q_{\max}^j \geq L_t \end{cases}$$

This merit order dispatch model aims to derive reasonable generation quantities for a diverse set of power plants. Importantly, the model ignores many operational constraints (e.g., ramp-up times and minimum generation constraints) and non-convexities in the plant's cost functions (e.g., ramp-up costs).

5 Forward and option contracts

This section defines the option and forward contracts the generator and LSE can buy. In electricity markets, forward and option contracts have delivery periods, typically a year, quarter, or month. The contract specifies a quantity of electricity, typically $(e.g., 1MWh)$, that has to be sold or bought every hour during the delivery period (Coulon et al., 2013).

Following Cramton et al. (2024) and Coulon et al. (2013), we derive hedging strategies for options and forwards that cover much more granular delivery periods. The granular periods allow market participants to tailor their forward and option positions to their seasonal and daily load patterns. Thereby, market participants can manage quantity risks more effectively. Moreover, incentives to bid competitively in the day-ahead market are stronger if forward and option quantities are linked to the expected load on an hourly level.

Therefore, we define a delivery period of M as a unique combination of year-month-hour-weekend/weekdays. For instance, market participants can purchase options and forwards covering all hourly periods that fall within $M =$"weekdays 3-4 pm in July 2019". In this paper, we simulate the optimal hedging strategies for all combinations of year-month-hour-weekend/weekdays in 2019. We initialize the simulation on $t =$ December 1, 2018 where the generator and the LSE take all hedging decisions. We assume $\overline{L}_t = \overline{X}_t = 0$, $log(G_t) = m_G$ at decision time t Coulon et al. (2013). Moreover, we set a risk-free interest rate of 2% and a high strike price for the call option of \$200/MWh. We set such a high strike price since the option should only cover the tail of the day-ahead price distributions (Cramton et al., 2024).

Since forward contracts do not involve upfront payments, we can derive the arbitrage-free

forward price $F(t, M)$ for all hours k that fall in delivery period M using the no-arbitrage relationship under a risk-neutral measure $\mathbb{Q}$ (Coulon et al., 2013).

$$F(t, M) = \mathbb{E}_t^{\mathbb{Q}}[P_{k \in M}]$$

Similarly, the arbitrage-free call option price for delivery period M with $k \in M$ is

$$V(t, M) = \mathbb{E}_t^{Q}\left[e^{-r(k-t)}(P_k - K)^+\right]$$

Coulon et al. (2013) derive closed-form solutions for the arbitrage-free prices using the parameters estimated in the regime-switching model. We calculate the forward and option prices numerically based on the distribution of the day-ahead prices that we simulated using the regime-switching models. We have to calculate the prices numerically for two reasons: First, we cap the day-ahead prices at $\$9,000$/MWh to make the simulated day-ahead prices consistent with observed prices in ERCOT. Second, we calculate the optimal quantities of forwards and options numerically using a distribution of simulated day-ahead prices. Since the day-ahead price distribution has long tails, we would need to draw extremely large samples to obtain day-ahead price distributions that are consistent and arbitrage-free with the closed-form option and forward prices implied by the regime-switching model. Drawing these large samples is computationally infeasible. Our numerical forward and option prices converge to the closed-form prices implied by the regime-switching models for large samples if we remove the $\$9,000$/MWh price cap.

Numerically, the arbitrage-free forward price in the delivery period M can simply be calculated as the mean of the simulated day-ahead prices in M. Figure 4 illustrates the forward prices for each combination of year- month-hour-weekend/weekdays in 2019. [4] Forward prices are below \$50/MWh for most hours. In a few afternoon peak hours during summer months, forward prices reach more than \$100/MWh since day-ahead prices are high on average and face large spikes during these hours.

[4] The forward prices are calculated from the perspective of $t = 12/01/2018$

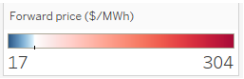

Hour	Year / Month 2019 Jan	Feb	Mar	Apr	May	Jun	Jul	Aug	Sep	Oct	Nov	Dec
0	21	21	22	23	24	26	27	27	25	24	22	22
1	19	19	19	19	21	23	24	24	22	20	20	20
2	19	18	17	17	18	21	23	23	21	19	18	19
3	20	19	18	17	18	20	22	22	20	19	19	20
4	22	22	20	19	19	20	22	22	21	20	20	22
5	28	28	26	23	22	22	23	23	23	23	25	27
6	52	52	43	33	27	25	25	26	28	31	37	46
7	50	50	43	34	28	26	26	27	28	31	36	44
8	42	42	38	33	29	28	28	28	29	30	34	39
9	38	39	37	33	31	30	30	31	31	31	33	35
10	34	36	35	34	33	34	35	35	34	32	31	33
11	31	33	35	35	37	40	43	43	40	34	31	30
12	29	31	34	37	42	48	54	54	47	37	31	28
13	27	31	36	41	50	64	79	82	66	44	32	27
14	26	30	37	46	63	93	134	142	99	54	32	26
15	25	31	41	57	89	154	247	268	168	71	35	25
16	26	33	45	67	111	189	286	304	194	83	39	27
17	47	44	45	53	74	105	124	114	90	70	59	53
18	58	62	59	52	51	56	66	70	63	53	49	52
19	40	49	56	55	50	47	50	55	55	48	40	37
20	35	42	50	53	50	47	46	46	45	39	34	32
21	31	34	36	37	38	39	40	39	36	33	31	30
22	27	29	30	31	32	33	34	33	31	29	28	27
23	24	25	25	26	27	29	30	29	28	26	25	24

Figure 4: Forward electricity prices for year-month-hour products for weekdays in 2019

The arbitrage-free price for the call option with strike price K =\$200/MWh for all hours $k \in M$ is given as

$$\begin{aligned} V(t,M) &= \mathbb{E}_t^Q \left[e^{-r(k-t)} (P_k - K)^+ \right] \\ &= \mathbb{E}_t^Q \left[e^{-r(k-t)} \underbrace{Prob(P_k > K)}_{\text{Spike frequency}} * \underbrace{E[P_k - K | P_k > K]}_{\text{Expected spike size}} \right] \end{aligned} \tag{11}$$

Figure 5 shows the option prices for the combinations of year-month-hour-weekend products. Option prices differ widely between products because the frequency and expected size of day-ahead price spikes differ by time of day and season. For instance, in a peak delivery period like Weekdays 4-5 pm in August 2019, day-ahead prices exceed the \$200/MWh strike price in 19% of simulated hourly periods and reach a maximum of \$9,000/MWh. In off-peak hours on Weekends, 1-2 am in July, the day-ahead price exceeds the day-ahead price in only 0.3% of the simulated hourly periods and reaches a far smaller maximum of \$426/MWh.

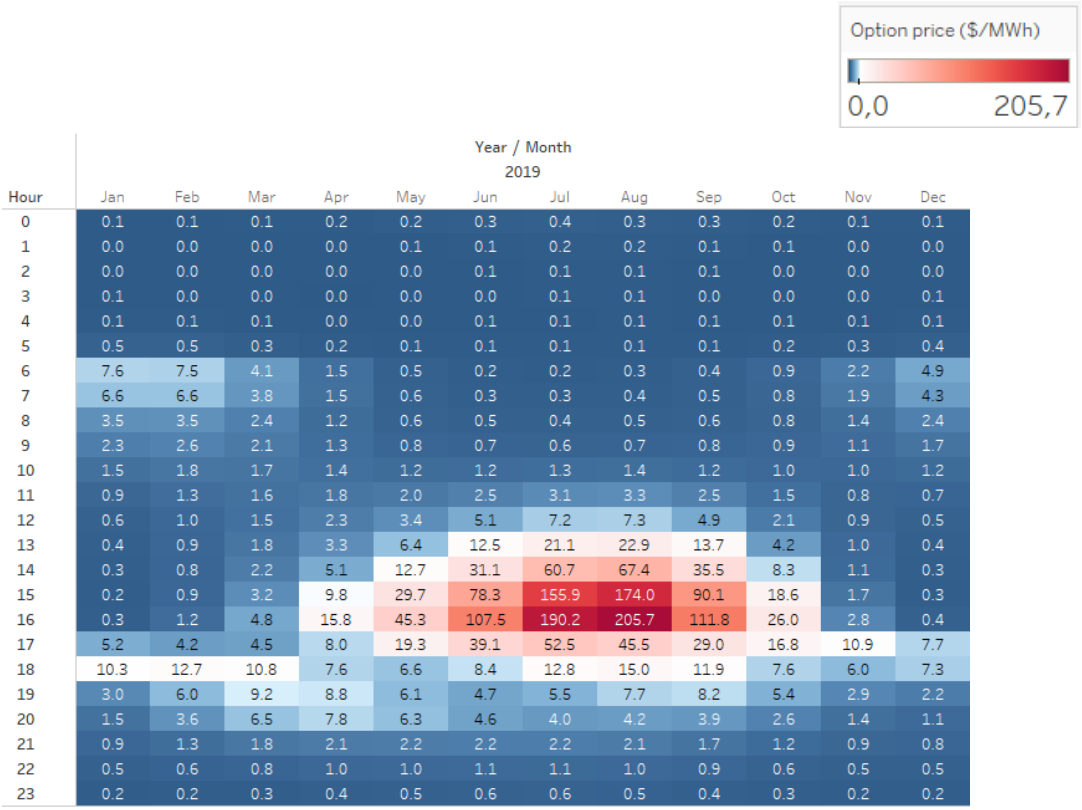

Hour	Jan	Feb	Mar	Apr	May	Jun	Jul	Aug	Sep	Oct	Nov	Dec
0	0.1	0.1	0.1	0.2	0.2	0.3	0.4	0.3	0.3	0.2	0.1	0.1
1	0.0	0.0	0.0	0.0	0.1	0.1	0.2	0.2	0.1	0.1	0.0	0.0
2	0.0	0.0	0.0	0.0	0.0	0.1	0.1	0.1	0.1	0.0	0.0	0.0
3	0.1	0.0	0.0	0.0	0.0	0.0	0.1	0.1	0.0	0.0	0.0	0.1
4	0.1	0.1	0.1	0.0	0.0	0.1	0.1	0.1	0.1	0.1	0.1	0.1
5	0.5	0.5	0.3	0.2	0.1	0.1	0.1	0.1	0.1	0.2	0.3	0.4
6	7.6	7.5	4.1	1.5	0.5	0.2	0.2	0.3	0.4	0.9	2.2	4.9
7	6.6	6.6	3.8	1.5	0.6	0.3	0.3	0.4	0.5	0.8	1.9	4.3
8	3.5	3.5	2.4	1.2	0.6	0.5	0.4	0.5	0.6	0.8	1.4	2.4
9	2.3	2.6	2.1	1.3	0.8	0.7	0.6	0.7	0.8	0.9	1.1	1.7
10	1.5	1.8	1.7	1.4	1.2	1.2	1.3	1.4	1.2	1.0	1.0	1.2
11	0.9	1.3	1.6	1.8	2.0	2.5	3.1	3.3	2.5	1.5	0.8	0.7
12	0.6	1.0	1.5	2.3	3.4	5.1	7.2	7.3	4.9	2.1	0.9	0.5
13	0.4	0.9	1.8	3.3	6.4	12.5	21.1	22.9	13.7	4.2	1.0	0.4
14	0.3	0.8	2.2	5.1	12.7	31.1	60.7	67.4	35.5	8.3	1.1	0.3
15	0.2	0.9	3.2	9.8	29.7	78.3	155.9	174.0	90.1	18.6	1.7	0.3
16	0.3	1.2	4.8	15.8	45.3	107.5	190.2	205.7	111.8	26.0	2.8	0.4
17	5.2	4.2	4.5	8.0	19.3	39.1	52.5	45.5	29.0	16.8	10.9	7.7
18	10.3	12.7	10.8	7.6	6.6	8.4	12.8	15.0	11.9	7.6	6.0	7.3
19	3.0	6.0	9.2	8.8	6.1	4.7	5.5	7.7	8.2	5.4	2.9	2.2
20	1.5	3.6	6.5	7.8	6.3	4.6	4.0	4.2	3.9	2.6	1.4	1.1
21	0.9	1.3	1.8	2.1	2.2	2.2	2.2	2.1	1.7	1.2	0.9	0.8
22	0.5	0.6	0.8	1.0	1.0	1.1	1.1	1.0	0.9	0.6	0.5	0.5
23	0.2	0.2	0.3	0.4	0.5	0.6	0.6	0.5	0.4	0.3	0.2	0.2

Figure 5: Option prices for year-month-hour products for weekdays for a spike price of $200/MWh in 2019

The primary channel through which day-ahead price spikes affect the optimal quantity of forwards and options is that price spikes change the relative prices of forwards and options. The three graphs in Figure 6 show the frequency of day-ahead price spikes ($Prob(P_k > K)$) on the x-axes and the expected spike size ($E[P_k - K|P_k > K]$) on the y-axes for all 576 year-month-hour-weekend/weekday delivery periods in 2019. The graphs reveal that there is a strong positive correlation between the frequency and the average size of spikes. The color shades highlight the arbitrage-free forward prices (graph 6a) and option prices (graph 6b) increase in spike frequency and size.

However, option prices rise much stronger in spike frequency and size than forward prices. As Equation 11 points out, option prices only depend on spike prices. In contrast, forward prices take the expectation across all day-ahead prices such that price spikes weaken the forward price price. Graph 6c highlights that the relative price ratio of option-to-forward prices increases in spike frequency and size. Therefore, the relative price ratio can be interpreted as a measure of the "spikiness" of the day-ahead price distribution because it is strongly correlated with spike frequency and size. In the following, we analyze how the spikiness of a delivery period, as measured by the option-to-forward price ratio, affects the demand for options and forwards.

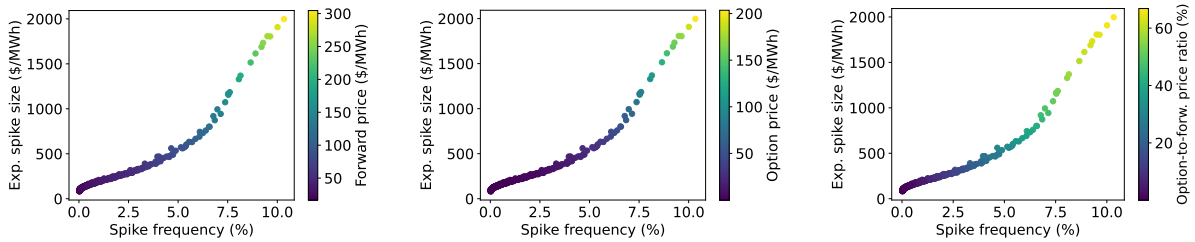

(a) Forwards prices (b) Option prices (c) Option-to-forwards price ratio

Figure 6: Forwards prices, option prices, and option-to-forwards price ratio for granular delivery periods by spike frequency and expected spike size

6 Optimal hedging strategies

In this section, we numerically simulate static optimal hedging strategies for a representative generator and a representative LSE. The generator mimics a large incumbent who owns 147 powerplants and a cumulative operating capacity of 34 GW. The plants were selected from our sample of power plants based on Mann et al. (2017) and ERCOT (2023) in order form a representative and diverse generation portfolio. Figure 7 shows the share of capacity by technology, highlighting that the generator is technologically diversified and owns plants with varying marginal costs. For each of the generator's power plants, we simulate hourly dispatch and profits using the merit order model in section 4.3.

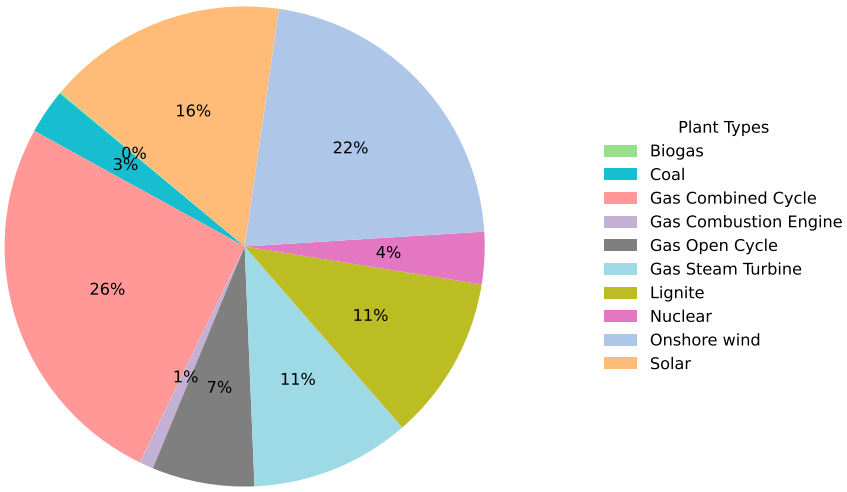

Figure 7: Share of technologies in the plant portfolio of a representative generator with 34 GW installed capacity

The LSE is assumed to serve on average 5% of the load in ERCOT. Its hourly load is imperfectly correlated with aggregate load (see section 4.3). The retail price equals the

average annual day-ahead price plus a 10% retail margin (Peura and Derek W. Bunn, 2021).

To isolate the distinct roles of forwards and options, we start deriving the optimal quantity of forwards only, assuming that options are not available. In section 6.2, we present hedging strategies that combine forwards and options.

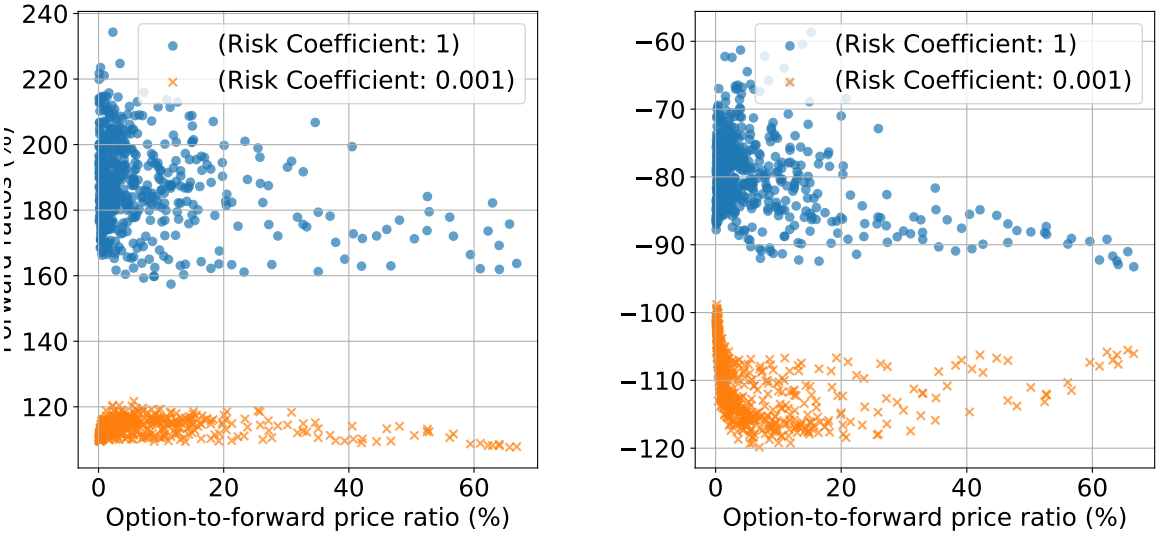

(a) LSE

(b) Generator

Figure 8: LSE and generator's optimal forward ratio by option-to-forward price ratio for delivery period weekdays 4-5 pm in August 2019

6.1 Hedging strategies with forwards only

We define a quantity of forward contracts as optimal if it maximizes the agent's expected utility for a given constant absolute risk aversion (CARA) coefficient. This optimal quantity is expressed as a forward hedge ratio, i.e., the optimal quantity of forward contracts as a percentage of the agent's expected load during the contract's delivery period. There are 576 unique granular year-month-hour-weekend/weekday delivery periods in 2019.

Figure 8a shows the optimal forward ratio for an LSE for all 576 delivery periods in 2019 as a function of the option-to-forward price ratio in each delivery period. The larger the option-to-forward price ratio, the larger the frequency and size of day-ahead price spikes in the delivery period. We show the hedge ratios for two levels of relative risk aversion: 0.001 and 1. A relative risk coefficient of 0.001 means that the LSE is almost risk neutral, while 1 implies strong risk aversion. Despite using a CARA utility function, we relate hedge ratios to relative risk aversion to make risk preferences comparable between agents

with different profit scales.[5]

Figures 8a reveals that the frequency and size of price tails have only a small impact on the optimal forward ratios for the LSE when only forwards are available. When the LSE is almost risk neutral with a risk coefficient of 0.01, the forward ratios are not sensitive to price spikes and vary between 108-122%. For a higher risk aversion of 1, the LSE's forward ratios slightly decline when day-ahead price tails become more severe. However, risk preferences are far more relevant for the LSE's forward ratios than price spikes. When the LSE dislikes risk with a risk coefficient of 1, it strongly overhedges with hedge ratios between 160-230%.

The generator's short forward position is also not sensitive to the frequency and size of price spikes for low risk aversion, as Figure 8b shows. The nearly risk neutral generator chooses short forward positions of 98-120% of expected generation. For high risk aversion of 1, the generator chooses smaller short positions of only 58-93% . Its short forward ratio is slightly higher in periods with heavier price spikes.

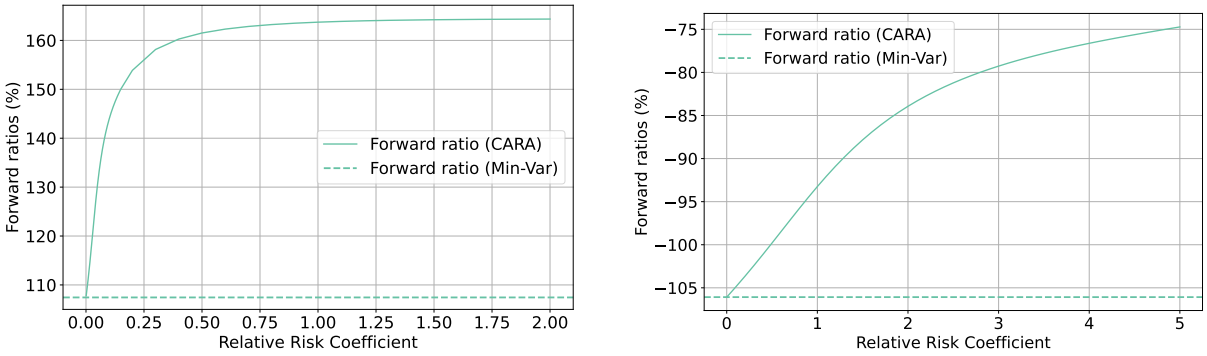

(a) LSE

(b) Generator

Figure 9: LSE and generator's optimal forward ratio by relative risk aversion for delivery period weekdays 4-5 pm in August 2019

To better understand how price spikes shape the above hedge strategies, we deep dive on

[5]Raskin and Cochran (1986) demonstrate that absolute risk aversion coefficients are hardly comparable between agents whose profits or wealth differs in scale. Assume agent A's profits fluctuate around an average of 100$ and agent B's profits fluctuate around 1000,000$. The CARA coefficient measures how the agents' marginal utility of profits changes when profits increase by an absolute amount, say 1$. Intuitively, a 1$ increase in profits should change A's marginal utility of profits much more than B's because the 1$ causes a much larger relative profit increase for A. To make risk preferences comparable between A and B, we select a risk preference expressed as a coefficient of relative risk aversion. When calculating hedge ratios, we first assume a relative risk parameter. Then, we divide this relative risk parameter by an agent's average profit during the hedge contract's delivery period. This transforms the relative risk parameter into an absolute risk parameter. The absolute and relative coefficients describe the same preferences at least locally at the agent's average profit. We assume this absolute risk parameter to be constant across profit levels (CARA). Hence, the CARA parameter represents the same preferences as the relative risk aversion coefficient locally at the agent's average profit. Expressing risk preferences in terms of relative risk in a CARA framework is common in the optimal hedge literature (Newbery (1989), Lapan and Moschini (1994)).

peak delivery period Weekdays 4-5 pm in August 2019. This peak delivery period has frequent and large price spikes, which is reflected in a high option-to-forward price ratio of 68%. Figure 9 shows the optimal forward ratios for this peak delivery period as a function of the agents' relative risk aversion. The forward ratios for a CARA utility maximizing LSE increase in risk aversion for low levels of relative risk aversion below 1 (Graph 9a). If risk aversion increases beyond 1, the hedge ratio remains constant. Irrespective of its risk aversion, the LSE wants to over the hedge, i.e., it wants to buy forward between 7%-64% more than its expected load. In contrast, the generator takes a short forward position that declines in risk aversion (Graph 9b). The generator's optimal hedge ratios are also more sensitive to increases in risk aversion, even for large risk coefficients.

As a comparison, the dashed line illustrates the optimal forward ratio if the agents want to minimize their profits' variance (Min-Var). For low-risk aversion, the CARA-optimal forward ratio equals the Min-Var forward ratio. The Min-Var ratio is a 106% short position for the generator and a 107% long position for the LSE. Hence, the generator and the LSE want to hedge roughly the opposite quantities if they are almost risk-neutral. The Min-Var hedge ratio requires agents to slightly over hedge, which indicates that their load is positively correlated with day-ahead prices (McKinnon (1967), Borenstein (2007)).

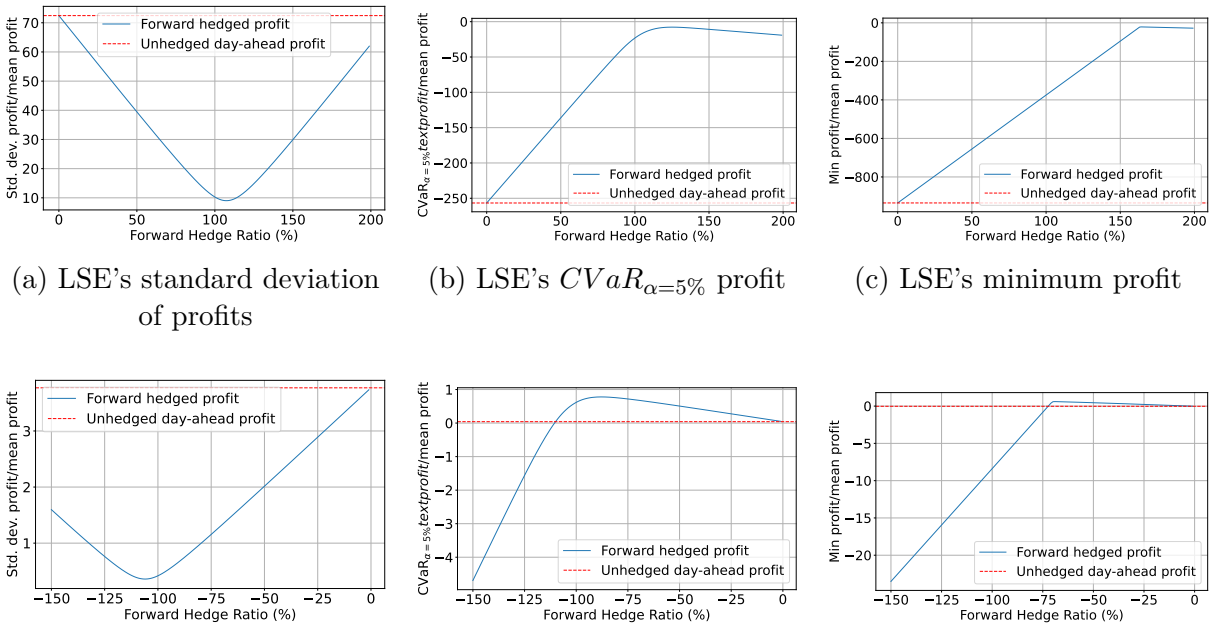

(a) LSE's standard deviation of profits

(b) LSE's $CVaR_{\alpha=5\%}$ profit

(c) LSE's minimum profit

(d) Generator's standard deviation of profits

(e) Generator's $CVaR_{\alpha=5\%}$ profit

(f) Generator's minimum profit

Figure 10: LSE and generator's profit standard deviation, ($CVaR_{\alpha=5\%}$) profit outcome, and minimum profit relative to mean unhedged day-ahead (DA) profit by forward ratio for delivery period Weekdays 4-5 pm in August 2019

To rationalize the above strategies, Figure 10 examines how the forward hedge ratio affects the LSE and generator's profit volatility, their conditional value at risk at the 5% level

($CVaR_{\alpha=5\%}$)[6], and worst-case minimum profit relative to their respective mean unhedged day-ahead profit. The average profit is not affected by the quantity of forwards since the forward price is arbitrage-free (Coulon et al., 2013).

Figure 10 highlights that agents' hedge strategies are driven by a trade-off between minimizing profit variance and maximizing worst-case tail outcomes. Both agents choose the Min-Var hedge ratio that minimizes profit variance if they are nearly risk-neutral. However, the generator's Min-Var ratio is a 106% short forward position, which leads to substantial negative tail losses as measured by a negative $CVaR_{\alpha=5\%}$ profit and negative minimum profit (Graphs 10e and 10f). A short position causes large losses when price spikes occur. The more the generator dislikes risk, the more it reduces the short position to avoid tail losses at the expense of an increase in profit variance (Graph 10a).

The risk-averse LSE also aims to reduce its tail losses by choosing a long forward position that exceeds its Min-Var position. The LSE needs to buy more than its expected quantity forward to be well protected against price spikes because spikes often occur when the load is above average. For high-risk aversion greater 1, the LSE chooses a hedge ratio of 164% because this ratio maximizes its worst-case minimum profit (Figure 14c). However, the worst-case minimizing ratio 164% leads to high tail losses $CVaR_{\alpha=5\%}$ and high-profit volatility. Yet, the profit volatility for a hedge ratio of 164% is still much lower than the profit volatility for an unhedged 0% hedge ratio as the dashed red line in Graph 10a reveals.

Noticeably, the LSE's $CVaR_{\alpha=5\%}$ tail loss is already minimized at a forward ratio of 125%. The reason for this large difference between the $CVaR_{\alpha=5\%}$ minimizing ratio and the worst-case minimizing ratio of 164% is that there are few extreme negative outliers in the LSE's day-ahead profit distribution. These outliers are so extreme that the LSE starts focusing primarily on these worst-case outliers, even for moderate risk aversion. In contrast, the generator does not exclusively focus on the minimum profit, even for high risk aversion. Its day-ahead profit distributions do not exhibit such large negative tails because the generator has more flexibility to shut down its plants when prices are unfavorable.

In appendix D we present forward hedging strategies for an off-peak period with small and rare price spikes: Weekends, 4 am in May 2019. Forward hedging strategies in the off-peak period look very similar to the peak period. When the LSE is very risk-averse,

[6] $CVaR_{\alpha=5\%}$ is the average of the lowest 5% of the profits in the profit distribution. Suppose profit π takes random values $\{\pi_1, \pi_2, \ldots, \pi_N\}$ with probabilities $\{p_1, p_2, \ldots, p_N\}$. Reorder these values such that $\pi_{(1)} \leq \pi_{(2)} \leq \ldots \leq \pi_{(N)}$ with corresponding probabilities $p_{(1)}, p_{(2)}, \ldots, p_{(N)}$. Let the partial sums be $P_{(k)} = \sum_{i=1}^{k} p_{(i)}$, for $k = 1, \ldots, N$. Define $\alpha = 0.05$ and find the smallest k such that $P_{(k)} \geq \alpha$. Then $\text{CVaR}_{\alpha=5\%} = \frac{1}{\alpha}\left[\sum_{i=1}^{k-1} \pi_{(i)}\, p_{(i)} + \pi_{(k)}\left(\alpha - P_{(k-1)}\right)\right]$ (Shapiro et al., 2021).

it chooses larger forward ratios in off-peak periods than in peak periods. The generator's hedge ratios are almost the same in peak and off-peak periods. Price spikes only have a small effect on hedge ratios when hedging with forwards only.

Overall, hedging with forwards only is surprisingly effective in reducing volatility and worst-case outcomes for a delivery period with extreme price spikes like Weekdays 4-5 pm in August 2019. The reason is that the generator and LSE's unhedged day-ahead market profit in the peak period is roughly a linear function of the day-ahead price as Figure 11 highlights[7]. One might have expected a strongly nonlinear relation between day-ahead prices and unhedged profits during a peak period since spike prices are often correlated with high load. However, Figure 20 in Appendix C reveals only a weak positive correlation between simulated load and prices for the peak delivery period Weekdays 4-5 pm in August 2019. In particular, very high spike prices are only slightly positively correlated with load. Spike prices likely depend much more on net load and random factors like outages than on load in modern electricity markets.

It is widely assumed that adding nonlinear options to a linear forward hedge strategy creates little benefits if profits are linear in prices and if forward and option prices are arbitrage-free (Lapan et al., 1991). In the following, we analyze whether options can still play a role in the generator and LSE's hedging strategy in the presence of large price spikes.

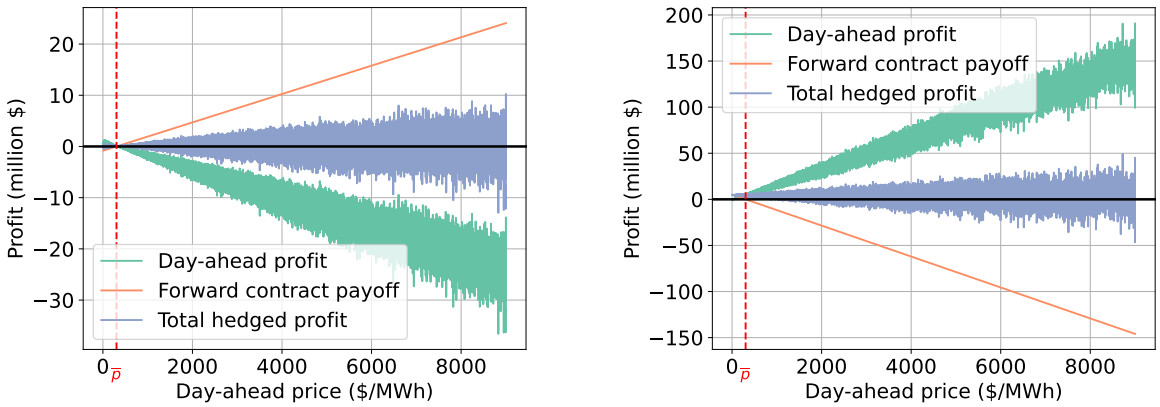

(a) LSE

(b) Generator

Figure 11: LSE and generator's day-ahead market profit, forward contract payoffs, and total hedged profit as a function of the day-ahead price for delivery period weekdays 4-5 pm in August 2019

[7]The forward contract payoff shown in Figure 11 is the payoff of a Min-Var hedge strategy chosen by a nearly risk neutral agent. The Min-Var hedge achieves the lowest profit variance by choosing a forward position that is roughly the opposite of the day-ahead position

6.2 Hedging with forwards and options

When combining forwards and options, hedging strategies become far more sensitive to severe price tails. Figures 12a and 12b present the optimal forward and option ratios for the LSE's combined hedging strategy for the 576 delivery periods in 2019 as a function of the delivery period's options-to-forward price ratio. A delivery period with a high options-to-forward price ratio has large and frequent price spikes. The LSE's forward ratios decline when a delivery period has more severe price spikes. The more risk-averse the LSE, the more sensitive its forward ratio to price tails.

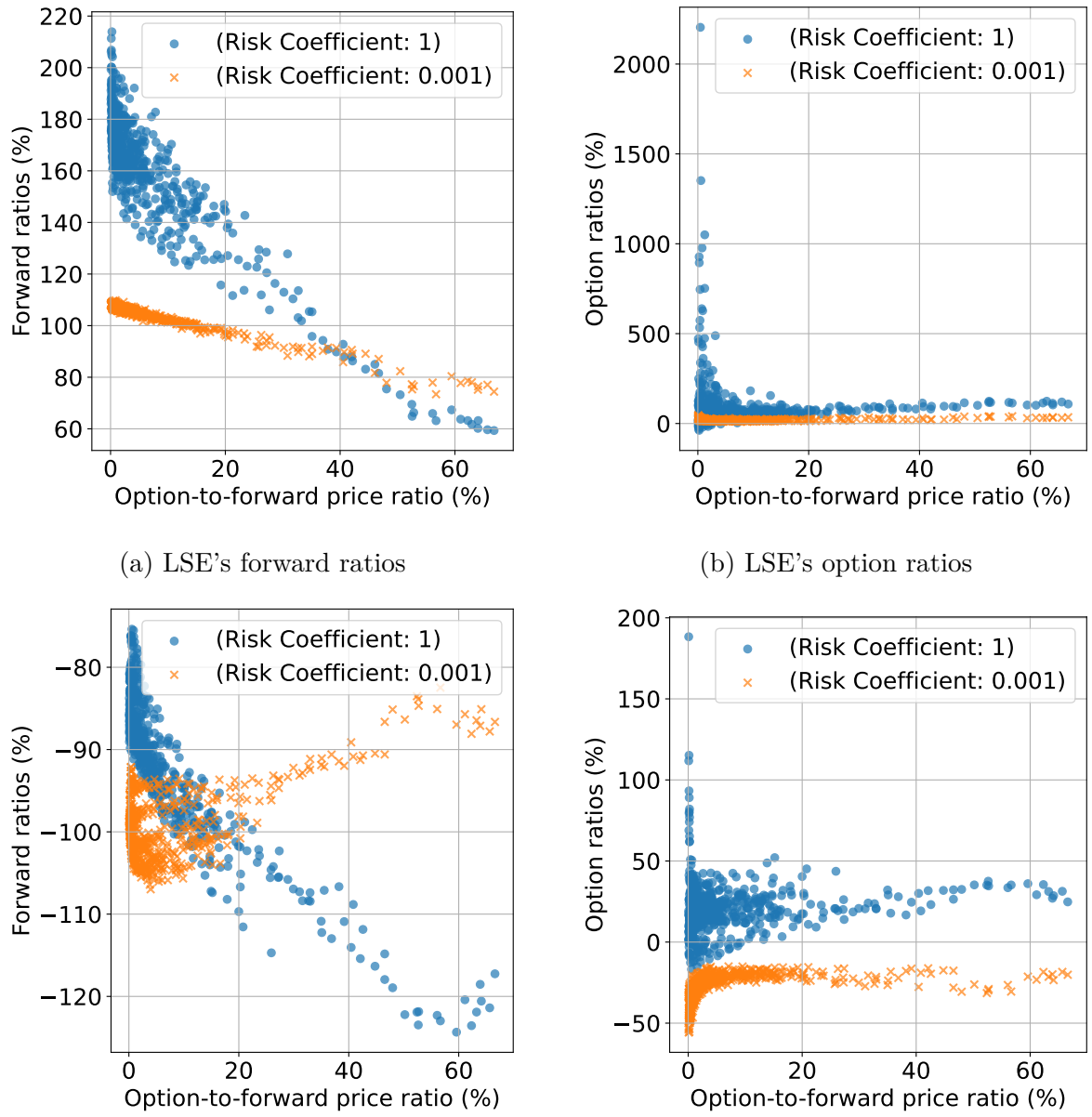

(a) LSE's forward ratios

(b) LSE's option ratios

(c) Generator's forward ratios

(d) Generator's option ratios

Figure 12: LSE and generator's optimal forward and option ratios by option-to-forward price ratio for delivery period weekdays 4-5 pm in August 2019

Figure 12b highlights that the option ratios for the almost risk-neutral LSE only slightly increase from 15-20% to 30-40% when day-ahead price distributions become spikier (relative risk coefficient 0.001). In the high risk aversion case (risk coefficient of 1), the LSEs selects much higher option ratios of 74-109% in spiky periods. In periods with rare and small price spikes, the LSE takes smaller option ratios for most periods. However, there are a few outlier periods in which the LSE selects large long positions or small short positions. In these periods, price spikes are extremely rare, and the option price is almost zero. A single extreme price spike can dominate the tail of the price distribution in such a

period. Therefore, the option ratio in these low-spike periods is sensitive to outliers in the simulated tail of the profit distribution and is not stable across repeated draws of profit distributions.

Overall, the risk-averse LSE chooses a higher option than forward ratios in periods with large price spikes. In contrast, the almost risk-neutral LSE relies more on forwards than options when price spikes are severe.

The generator's short forward position declines in the option-to-forward price ratio for small risk aversion (0.001) as Figures 12c illustrates. For large risk aversion (1), the short forward position increases in price spikiness. Analogously to the LSE, the almost risk-neutral generator takes only small short positions in options, mainly around 20% with a few larger outliers (Figure 12d). The short option position remains small if the day-ahead price distribution becomes spikier. The risk-averse generator (1) chooses almost exclusively long option positions, mostly around 20-40%. These long positions slightly increase when price spikes are large and frequent.

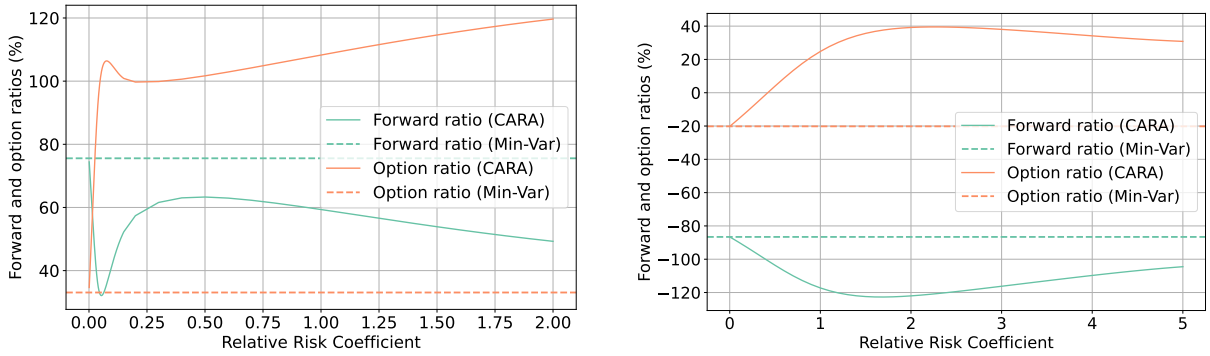

(a) LSE (b) Generator

Figure 13: LSE and generator's optimal forward and option ratio by relative risk aversion for delivery period weekdays 4-5 pm in August 2019

We deep dive again on peak delivery period weekdays 4-5 pm in August 2019. Figure 13a shows the LSE's optimal forward and option ratios across risk-aversion levels. For this peak period, the importance of options in the LSE's hedging strategy increases relative to forwards when the LSE becomes more risk-averse. As mentioned above, when the CARA minimizing LSE is almost risk-neutral, it buys the number of forwards and options that minimize the variance of profits (Min-Var). The Min-Var hedge position buys options and forwards roughly in the ratio 2:1. Buying 2 call options and 1 forward contract replicates the payoff of a long straddle. A long straddle position is known to be effective for reducing profit variance (Lapan et al., 1991).

The optimal option ratio rapidly increases in the LSE's risk aversion. The forward ratio also sharply declines for low-risk aversion. However, the forward ratios increase for inter-

mediate risk aversion and decline afterward. The LSE's forward ratios are less sensitive to risk preferences than option ratios. The LSE starts buying more options than forwards in this peak delivery period, even for small levels of risk aversion.

For the generator, Figure 13b highlights that the almost-risk neutral generator takes a minimum variance (Min-Var) strategy that is similar to the LSE's strategy but with opposite signs since the generator goes short in forwards and options. The generator slightly increases its short position in forwards for intermediate risk levels. At the same time, the short option position decreases more strongly. The generator's option position transitions to a long position for larger risk aversion.

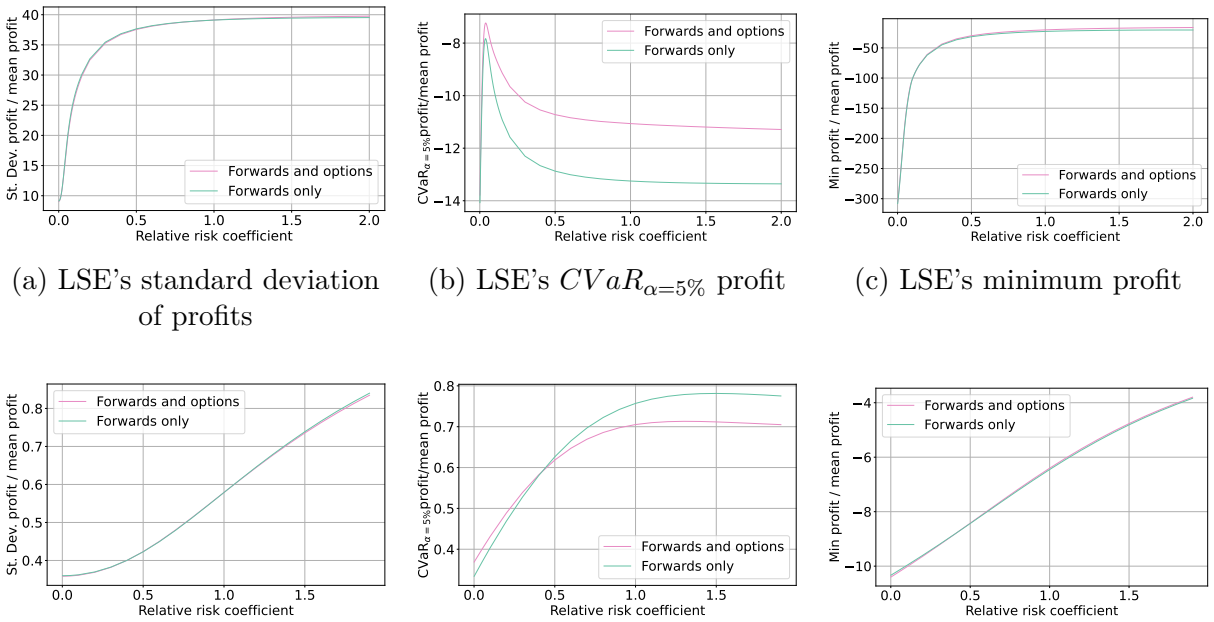

(a) LSE's standard deviation of profits

(b) LSE's $CVaR_{\alpha=5\%}$ profit

(c) LSE's minimum profit

(d) Generator's standard deviation of profits

(e) Generator's $CVaR_{\alpha=5\%}$ profit

(f) Generator's minimum profit

Figure 14: LSE and generator's profit standard deviation, minimum and maximum profit relative to mean unhedged day-ahead (DA) profit by relative risk aversion level for delivery period Weekdays 4–5 pm in August 2019

The pink line in figures 14 depicts the agents' standard deviation of profits, $CVaR_{\alpha=5\%}$ tail loss, and worst-case minimum loss as a function of the optimal forward and option ratios that are associated with a relative risk aversion level. For instance, at a risk coefficient of 0.001, the LSE chooses a 76% forwards ratio and 32% options ratio because this Min-Var portfolio leads to the lowest standard deviation of its profits (Graph 14a). The nearly risk-averse generator also chooses the Min-Var hedge portfolio (Graph 14d)).

For small risk aversion, both agents focus more on improving the $CVaR_{\alpha=5\%}$ lowest profit outcomes, which comes at the expense of larger profit variance. The LSE can reduce the $CVaR_{\alpha=5\%}$ tail loss by buying more options and fewer forwards. Going long in options protects more effectively from price spikes than forwards. The generator protects from

price spikes by gradually turning its short option position into a long one. Going long in options has the disadvantage of increasing the generator's profit variance because the long option has a high payoff when the generator's day-ahead profits are high anyway. The generator balances the long option position with a larger short forward position to limit the increase in variance.

The more risk-averse the generator and LSE become, the more they focus on ever more extreme parts of the lower end of their profit distribution. The highly risk-averse LSE buys even more options to reduce the minimum worst-case loss at the expense of a larger $CVaR_{\alpha=5\%}$ tail loss. The generator also reduces its long option and short forward positions to achieve a marginal increase in its lowest worst-case profit.

Figure 14 also reveals that the combined forwards and options strategy (pink line) add only limited value compared to the optimal forwards-only strategy (green line). Compared to the forwards-only strategy, the combined strategy achieves only tiny improvements in profit standard deviation and minimum loss. The improvements in terms of $CVaR_{\alpha=5\%}$ tail outcomes are more substantial, but these improvements seem negligible compared to the improvements achieved relative to the unhedged day-ahead $CVaR_{\alpha=5\%}$ outcome as Figure 25 in Appendix E reveals. As discussed above, the forwards-only strategy achieves excellent results thanks to the linear relationship between day-ahead prices and profits. Even though options do not add large benefits, the agents still take significant option positions when they are risk-averse because the option achieves small improvements in the tail and worst-case profits. These small improvements can cause large utility increases for risk-averse agents.

Overall, Figure 25 in Appendix E shows that the combined strategy and the forwards-only strategy achieve enormous reductions in profit variance, $CVaR_{\alpha=5\%}$ tail loss, and worst-case loss compared to the case when the LSE trades fully unhedged in the day-ahead market. Compared to remaining unhedged, hedging with either forwards-only or combining forwards and options proves effective in managing tail risks and profit variance.

In appendix D, we also examine the optimal combined forwards and options strategy for off-peak period Weekends 4-5 am in May 2019, which has small and rare spike price. Compared to the peak period, the LSE relies far less on long option positions and chooses larger forward quantities in the off-peak period (see Figure 23). The generator also chooses only very small long option positions for moderate risk levels and small short option ratios for high risk aversion. Choosing small long option or even short option position allows the generator to reduce its short forward position for high risk levels in the off-peak periods. This contrasts with the above peak period, where the risk-averse generator selects long option and large short forward positions. In the off-peak period, the combined hedge strategy is more effective in reducing profit variance and the $CVaR_{\alpha=5\%}$ loss compared to the forwards-only strategy as Figure 24 emphasizes. The combined strategy only

marginally improves worst-case minimum outcomes for high risk levels relative to the forwards-only approach.

6.3 Hedging and option strike prices

In the next section, we analyze how the demand for forwards and options change, if we choose a different strike price for the call option. So far, we set the strike price to $\$200/MWh$ such that the option covers only the extreme tails of the price distribution. Choosing a lower strike price makes the option more valuable relative to the forward since the option is more frequently in the money if the strike price is low. The higher option value is reflected in a higher arbitrage-free option price.

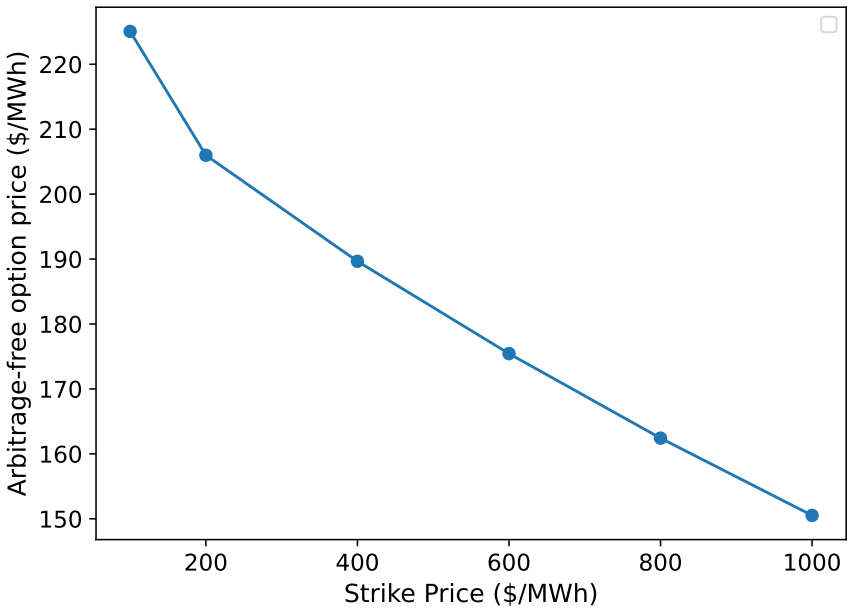

Figure 15: Arbitrage-free option price as a function opf the call option's strike price for delivery period weekdays 4-5 pm in August 2019

Figure 15 shows the arbitrage-free option price as a function of the strike price for peak delivery period weekdays 4-5 pm in August 2019. The negative relation between option and strike price slightly diminishes in the strike price. The option price is high even for a large strike price of $\$1,000$/MWh. The reason is that there is a low probability of 6% that the simulated day-ahead prices exceed the high $\$1,000$/MWh strike price but a high expected spike size of $\$2,648$/MWh. In contrast, if the strike price is only \$100/MWh, the spike probability rises to 38% but the expected spike size is only \$590/MWh. This small average spike size explains why the \$100/MWh strike price option has only a moderately higher value than the option with a $\$1,000$/MWh strike price. For off-peak delivery

periods, a high \$1,000/MWh strike price leads to an option price of zero since the option will never be in the money for such a high strike price.

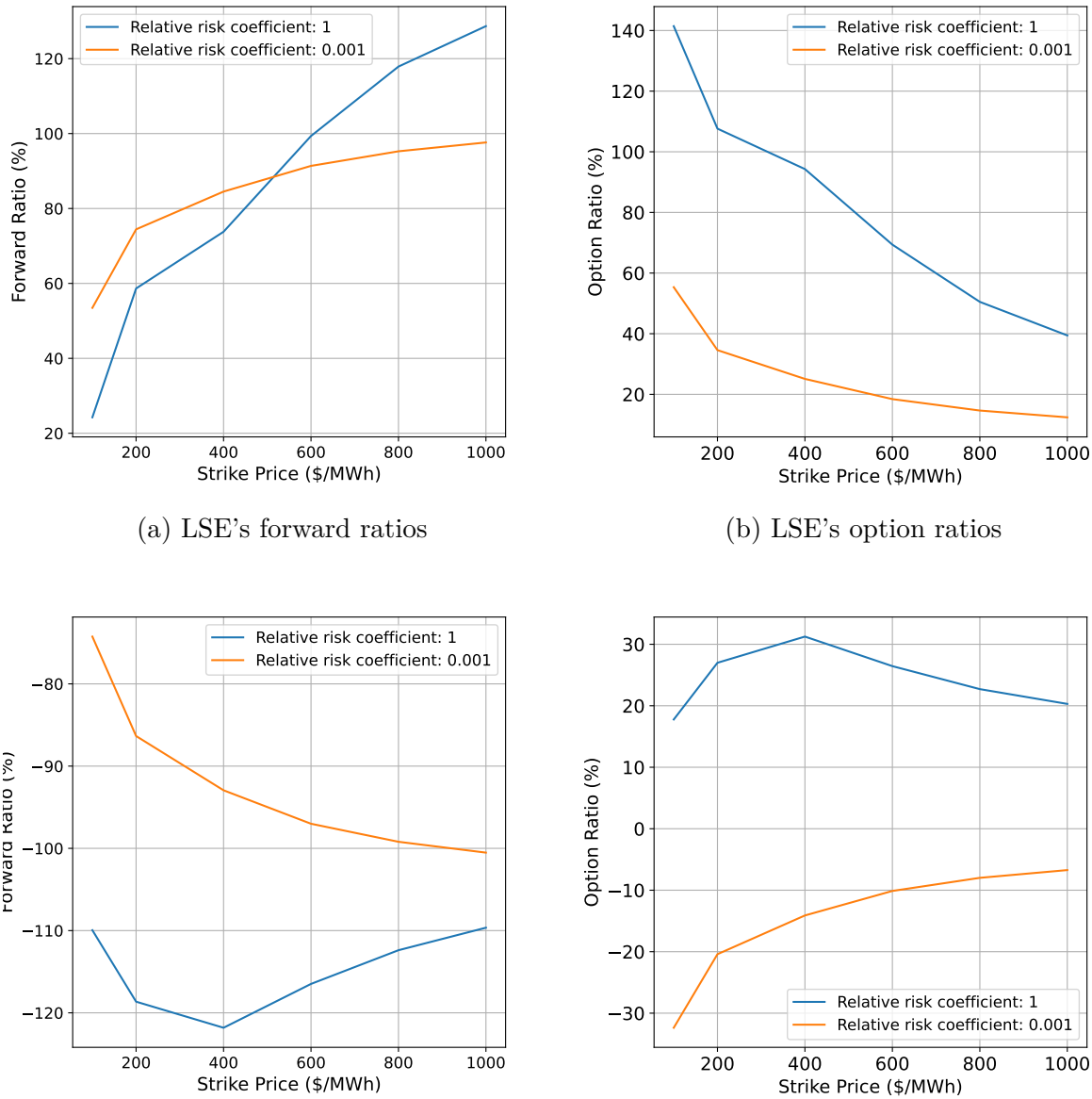

(a) LSE's forward ratios

(b) LSE's option ratios

(c) Generator's forward ratios

(d) Generator's option ratios

Figure 16: LSE and generator's optimal forward and option ratios by option strike price for delivery period weekdays 4-5 pm in August 2019

Figure 16 depicts the generator and LSE's forward and option ratios as a function of the call option's strike price for different risk preferences for peak delivery period weekdays 4-5 pm in August 2019. The LSE buys more forwards and fewer options when the strike price increases. The option becomes less effective in protecting the LSE from price spikes if the strike price is high. The more risk-averse the LSE, the more sensitive its forward

and option demand to higher strike prices.

The generator also sells more forwards and fewer options when the strike price is high for low-risk aversion (0.001). In contrast, for high-risk aversion (1), the generator's short forward position and its long option position decline when the strike price is large.

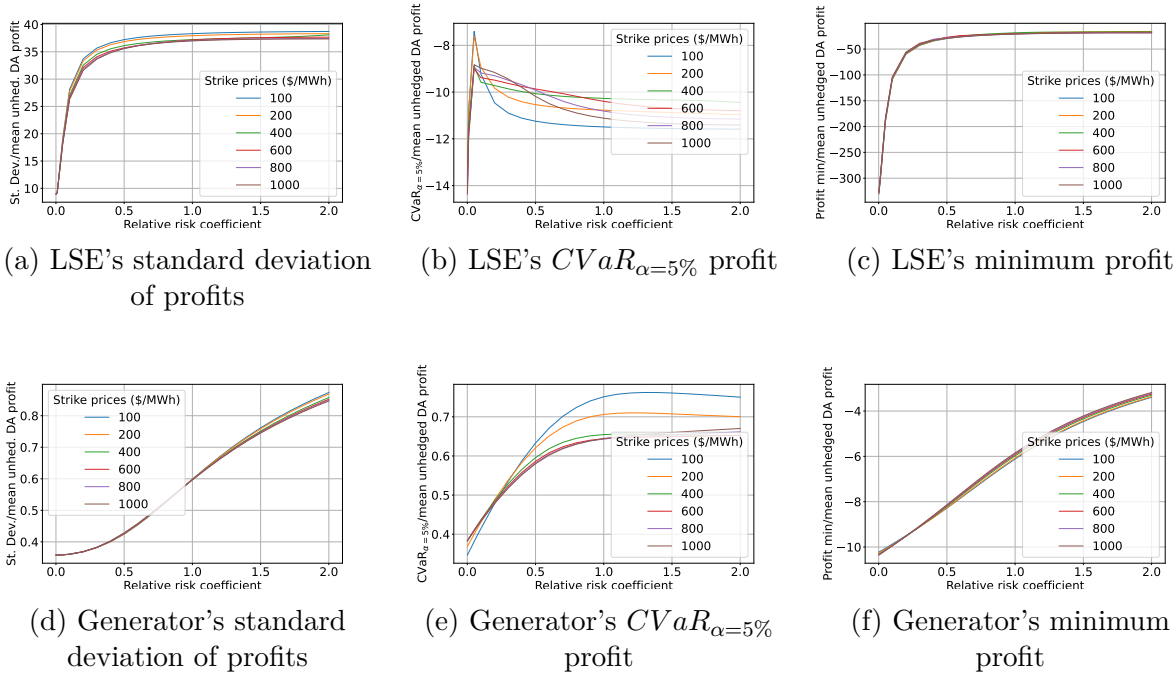

(a) LSE's standard deviation of profits

(b) LSE's $CVaR_{\alpha=5\%}$ profit

(c) LSE's minimum profit

(d) Generator's standard deviation of profits

(e) Generator's $CVaR_{\alpha=5\%}$ profit

(f) Generator's minimum profit

Figure 17: LSE and generator's profit standard deviation, minimum and maximum profit relative to mean unhedged day-ahead (DA) profit by relative risk aversion level for delivery period Weekdays 4–5 pm in August 2019 for different strike prices

Figures 17 shows the standard deviation of profits, $CVaR_{\alpha=5\%}$ tail outcome, and worst-case-minimum profit as a function of the agent's optimal combination of forwards and options that are linked to a relative risk aversion level for different strike prices. If the strike price is low, agents standard deviation of profits is larger compared to higher strike prices, especially for high risk levels (Graphs 17a and 17d). This higher standard deviation is caused by the large option positions the agents hold when strike prices are small. However, the differences in profit standard deviation and minimum worst-case profits (Graphs 17c and 17f) among different strike prices are small.

For the LSE, small strike prices lead to small $CVaR_{\alpha=5\%}$ tail losses for small risk aversion levels and high $CVaR_{\alpha=5\%}$ losses for high risk aversion (Graph 17b). By contrast, small strike prices lead to smaller positive $CVaR_{\alpha=5\%}$ profits for the nearly risk-neutral generator and substantially higher $CVaR_{\alpha=5\%}$ profits for the risk averse generator 17f. Hence, it depends on the risk preferences of market participants whether high or low strike prices provide better protection.

7 Conclusion

Day-ahead electricity markets exhibit extreme price fluctuations and sudden price spikes. The price spikes are often positively correlated with load. The positive correlation between load and price spikes poses substantial financial risk for load-serving entities (LSEs) because they have to sell large quantities at extremely high prices and sell the electricity at much lower prices to end-consumers. For generators, price spikes create upside opportunities but substantially increase the variance of profits. Generators and LSEs might, therefore, want to hedge parts of their profits.

In this paper, we derive optimal hedging strategies for a representative generator and an LSE in the ERCOT day-ahead market in Texas. We let the generator and the LSE choose the optimal portfolio of a forward contract and a call option that maximizes their constant absolute risk aversion utility function. Our research addresses the question of how price spikes, risk aversion, and option strike prices jointly shape the selection of forward and call option contracts.

To obtain realistic profit distributions, we first simulate hourly day-ahead prices and aggregate load under a regime-switching model for the Texas ERCOT market based on Coulon et al. (2013). We then apply a merit order dispatch model to simulate hourly generation quantities for a large sample of power plants. Afterward, we define 576 granular delivery periods for the option and forward contracts for each unique combination of year-month-hour-weekend/weekday in 2019. We find that the frequency and size of day-ahead price spikes differ widely between these delivery periods. This allows us to examine how different levels of spikiness in the day-ahead price distribution alter hedge choices for different delivery periods.

We compare the performance of various hedge portfolios, including forwards-only and mixed portfolios of forwards and call options, under differing levels of risk aversion and strike prices. Our results indicate that agents with low-risk aversion primarily rely on forward contracts, adding modest option positions. More risk-averse participants take larger long-option positions to protect their worst-case outcomes.

Surprisingly, the additional risk protection from combining forwards and options remains limited. Using options adds small extra value in terms of reducing variance and improving worst-case outcomes because the generator and the LSE's day-ahead market profits are roughly linear in the day-ahead price. Combined with linear forward contracts, nonlinear options achieve little additional benefits in terms of risk hedging when profits are linear (Lapan et al., 1991). Risk-averse agents still take long option positions because even small improvements in worst-case outcomes can raise utility when risk aversion is high.

Lastly, we show that a higher option strike price induces the generator and the LSE to

rely more on forward contracts and less on options. When the strike price is high, the option offers limited protection from relatively high prices that are below the strike price. Therefore, agents shift their portfolio from options to forwards.

Overall, our paper highlights that forwards and option contracts can effectively reduce financial risks for a generator and an LSE in the ERCOT day-ahead market in terms of profit variance and worst-case tail losses. We emphasize that we derived our optimal hedge strategies under the assumption of arbitrage-free prices. It would be interesting to analyze how arbitrage opportunities that often occur in electricity markets affect optimal hedging strategies. In forward markets, positive price premia occur in peak demand delivery periods with high price spikes (Redl et al. (2009), D. W. Bunn (2006)). These positive risk premia might hinder LSEs from buying sufficient forwards and option contracts to effectively hedge their large tail risks during peak delivery periods.

Therefore, policymakers should implement measures to reduce price premia in forwards and option markets to facilitate hedging and risk management. Price premia are partly driven by a lack of liquidity in these markets (Bevin-McCrimmon et al., 2018). Policymakers could increase market liquidity by fostering the use of centralized markets for forwards and options with centrally defined delivery periods. They might even oblige LSE to purchase forward a certain share of their expected demand to increase market liquidity. Price premia could also be reduced by facilitating the participation of financial institutions in forwards and options markets to increase arbitrage and improve price discovery (Cramton et al., 2024).

The above measures might make hedging in day-ahead markets an even more effective risk management tool for electricity generators and LSEs. When market participants are well hedged, the enormous risk inherent in day-ahead electricity markets is carried on many shoulders. Hedging enables market participants to deal with extreme price spikes that are necessary as scarcity signals in short-term power markets.

References

Afanasyev, D. O., Fedorova, E. A., & Popov, V. U. (2015). Fine structure of the price–demand relationship in the electricity market: Multi-scale correlation analysis. *Energy Economics*, *51*, 215–226. https://doi.org/10.1016/j.eneco.2015.07.011

Aïd, R., Campi, L., & Langrené, N. (2013). A structural risk–neutral model for pricing and hedging power derivatives. *Mathematical Finance: An International Journal of Mathematics, Statistics and Financial Economics*, *23*(3), 387–438. https://doi.org/10.1111/j.1467-9965.2011.00507.x

Allaz, B., & Vila, J.-L. (1993). Cournot competition, forward markets and efficiency. *Journal of Economic Theory*, *59*(1), 1–16. https://doi.org/10.1006/jeth.1993.1001

Azevedo, F., Vale, Z. A., & de Moura Oliveira, P. B. (2007). A decision-support system based on particle swarm optimization for multiperiod hedging in electricity markets. *IEEE Transactions on Power Systems*, *22*(3), 995–1003. https://doi.org/10.1109/TPWRS.2007.901463

Barbi, M., & Romagnoli, S. (2018). Skewness, basis risk, and optimal futures demand. *International Review of Economics & Finance*, *58*, 14–29. https://doi.org/10.1016/j.iref.2018.02.021

Barlow, M. T. (2002). A diffusion model for electricity prices. *Mathematical Finance: An International Journal of Mathematics, Statistics and Financial Economics*, *12*(4), 287–298.

Bessembinder, H., & Lemmon, M. L. (2002). Equilibrium pricing and optimal hedging in electricity forward markets. *the Journal of Finance*, *57*(3), 1347–1382.

Bevin-McCrimmon, F., Diaz-Rainey, I., McCarten, M., & Sise, G. (2018). Liquidity and risk premia in electricity futures. *Energy Economics*, *75*, 503–517. https://doi.org/10.1016/j.eneco.2018.09.002

Bhattacharya, S., Gupta, A., Kar, K., & Owusu, A. (2020). Risk management of renewable power producers from co-dependencies in cash flows. *European Journal of Operational Research*, *283*(3), 1081–1093.

Borenstein, S. (2007). Wealth transfers among large customers from implementing real-time retail electricity pricing. *The Energy Journal*, *28*(2), 131–149. https://doi.org/10.5547/ISSN0195-6574-EJ-Vol28-No2-6

Botterud, A., Kristiansen, T., & Ilic, M. D. (2010). The relationship between spot and futures prices in the nord pool electricity market. *Energy Economics*, *32*(5), 967–978. https://doi.org/10.1016/j.eneco.2009.11.009

Brandkamp, S. (2023). Hedging households against extreme electricity prices. *University of Cologne Working Paper*.

Bunn, D. W. [D. W.]. (2006). Risk and electricity price dynamics. *Platts. com News Feature*.

Carmona, R., Coulon, M., & Schwarz, D. (2013). Electricity price modeling and asset valuation: A multi-fuel structural approach. *Mathematics and Financial Economics*, *7*, 167–202.

Conejo, A., García, R., Carrion, M., Caballero, A., & Andres, A. (2008). Optimal involvement in futures markets of a power producer. *Power Systems, IEEE Transactions on*, *23*, 703–711. https://doi.org/10.1109/TPWRS.2008.919245

Coulon, M., Powell, W. B., & Sircar, R. (2013). A model for hedging load and price risk in the texas electricity market. *Energy Economics*, *40*, 976–988. https://doi.org/10.1016/j.eneco.2013.05.020

Cox, J. C., & Rubinstein, M. (1985). Options markets.

Cramton, P., Brandkamp, S., Chao, H.-p., Dark, J., Hoy, D., Kyle, A. S., Malec, D., Ockenfels, A., & Wilkens, C. (2024). A forward energy market to improve resiliency. https://cramton.umd.edu/electricity/

Cramton, P., MacKay, D. J. C., Ockenfels, A., & Stoft, S. (2017). *Global carbon pricing*. MIT Press.

Danthine, J.-P. (1978). Information, futures prices, and stabilizing speculation. *Journal of Economic Theory*, *17*(1), 79–98. https://doi.org/10.1016/0022-0531(78)90124-2

de Jong, C., & Huisman, R. (2002). Option formulas for mean-reverting power prices with spikes. *Energy Global Research Paper*.

Deng, S.-J., & Oren, S. S. (2006). Electricity derivatives and risk management. *Energy*, *31*(6-7), 940–953.

Deng, T., Yan, W., Nojavan, S., & Jermsittiparsert, K. (2020). Risk evaluation and retail electricity pricing using downside risk constraints method. *Energy*, *192*, 116672. https://doi.org/10.1016/j.energy.2019.116672

Dionne, G., & Santugini, M. (2015). Production flexibility and hedging. *Risks*, *3*(4), 543–552. https://doi.org/10.3390/risks3040543

Energy Information Administration. (2018). Electric power annual 2017. https://www.connaissancedesenergies.org/sites/connaissancedesenergies.org/files/pdf-pt-vue/electric_power_annual_2017.pdf

Energy Information Administration. (2023). Electric power monthly 2022.

Energy Information Administration. (2024). Henry hub natural gas spot price. https://www.eia.gov/dnav/ng/hist/rngwhhdD.htm

ERCOT. (2022). 2022 wind and solar profiles update. https://www.ercot.com/files/docs/2022/08/27/4___Updated_Wind_and_Solar_Production_Profiles.pptx

ERCOT. (2023). Ercot wind profiles and solar pv profiles, 1980-2022.

ERCOT. (2024a). Historical dam load zone and hub prices. https://www.ercot.com/mp/data-products/data-product-details?id=np4-180-er

ERCOT. (2024b). Hourly load data archives. https://www.ercot.com/gridinfo/load/load_hist

ERCOT. (2024c). Interval generation by fuel reports (2011-22). https://www.ercot.com/gridinfo/generation

Eydeland, A., & Geman, H. (1999). Fundamentals of electricity derivatives. *Energy Modelling and the Management of Uncertainty*, 35–43.

Fanelli, V., Maddalena, L., & Musti, S. (2016). Asian options pricing in the day-ahead electricity market. *Sustainable cities and society*, *27*, 196–202.

Feder, G., Just, R. E., & Schmitz, A. (1980). Futures markets and the theory of the firm under price uncertainty. *The Quarterly Journal of Economics*, *94*(2), 317–328. https://doi.org/10.2307/1884543

Füss, R., Mahringer, S., & Prokopczuk, M. (2015). Electricity derivatives pricing with forward-looking information. *Journal of Economic Dynamics and Control*, *58*, 34–57. https://doi.org/10.1016/j.jedc.2015.05.016

Hambly, B., Howison, S., & Kluge, T. (2008). Modelling spikes and pricing swing options in electricity markets. *Quantitative Finance*, 1–25.

Hamilton, J. D. (1990). Analysis of time series subject to changes in regime. *Journal of Econometrics*, *45*(1-2), 39–70.

Hess, M. (2021). Optimal hedging strategies for options in electricity futures markets. *Available at SSRN 3825720*.

Holthausen, D. M. (1979). Hedging and the competitive firm under price uncertainty. *American Economic Review*, *69*(5), 989–995.

Jin, H. J. (2007). Heavy–tailed behavior of commodity price distribution and optimal hedging demand. *Journal of Risk and Insurance*, *74*(4), 863–881. https://doi.org/10.1111/j.1539-6975.2007.00238.x

Ketterer, J. C. (2014). The impact of wind power generation on the electricity price in germany. *Energy Economics*, *44*, 270–280. https://doi.org/10.1016/j.eneco.2014.04.003

Kettunen, J., Salo, A., & Bunn, D. W. (2009). Optimization of electricity retailer's contract portfolio subject to risk preferences. *IEEE Transactions on Power Systems*, *25*(1), 117–128.

Lapan, H., & Moschini, G. (1994). Futures hedging under price, basis, and production risk. *American Journal of Agricultural Economics*, *76*(3), 465–477. https://doi.org/10.2307/1243658

Lapan, H., Moschini, G., & Hanson, S. D. (1991). Production, hedging, and speculative decisions with options and futures markets. *American Journal of Agricultural Economics*, *73*(1), 66–74.

Lee, Y., & Oren, S. S. (2009). An equilibrium pricing model for weather derivatives in a multi-commodity setting. *Energy Economics*, *31*(5), 702–713.

Lien, D. (2010). The effects of skewness on optimal production and hedging decisions: An application of the skew–normal distribution. *Journal of Futures Markets: Futures, Options, and Other Derivative Products*, *30*(3), 278–289.

Losq, E. (1982). Hedging with price and output uncertainty. *Economics Letters*, *10*(1-2), 65–70. https://doi.org/10.1016/0165-1765(82)90117-3

Lu, X., Dong, Z. Y., & Li, X. (2005). Electricity market price spike forecast with data mining techniques. *Electric Power Systems Research*, *73*(1), 19–29. https://doi.org/10.1016/j.epsr.2004.06.002

Mann, N., Tsai, C.-H., Gülen, G., Schneider, E., Cuevas, P., Dyer, J., Butler, J., Zhang, T., Baldick, R., & Deetjen, T. (2017). Capacity expansion and dispatch modeling: Model documentation and results for ercot scenarios. *The Full Cost of Electricity. The University of Texas at Austin Energy Institute*.

Matsumoto, T., & Yamada, Y. (2021). Simultaneous hedging strategy for price and volume risks in electricity businesses using energy and weather derivatives. *Energy Economics*, *95*, 105101.

McKinnon, R. I. (1967). Futures markets, buffer stocks, and income stability for primary producers. *Journal of political economy*, *75*(6), 844–861. https://doi.org/10.1086/259363

Moschini, G., & Lapan, H. (1992). Hedging price risk with options and futures for the competitive firm with production flexibility. *International Economic Review*, 607–618. https://doi.org/10.2307/2527128

Moschini, G., & Lapan, H. (1995). The hedging role of options and futures under joint price, basis, and production risk. *International Economic Review*, *36*(4), 1025. https://doi.org/10.2307/2527271

Näsäkkälä, E., & Keppo, J. (2005). Electricity load pattern hedging with static forward strategies. *Managerial Finance*, *31*(6), 116–137. https://doi.org/10.1108/03074350510769721

Newbery, D. M. (1989). Futures markets, hedging and speculation. In *Finance* (pp. 145–152). Springer.

Ocakoglu, K., & Tolga A. (2018). Effective trading in turkish electricity market: Hedging with options. *Proceedings of the World Congress on Engineering*.

Oum, Y., Oren, S., & Deng, S. (2006). Hedging quantity risks with standard power options in a competitive wholesale electricity market. *Naval Research Logistics (NRL)*, *53*(7), 697–712.

Oum, Y., & Oren, S. S. (2010). Optimal static hedging of volumetric risk in a competitive wholesale electricity market. *Decision Analysis*, *7*(1), 107–122. https://doi.org/10.1287/deca.1090.0167

Peura, H., & Bunn, D. W. [Derek W.]. (2021). Renewable power and electricity prices: The impact of forward markets. *Management Science*, *67*(8), 4772–4788.

Raskin, R., & Cochran, M. J. (1986). Interpretations and transformations of scale for the pratt-arrow absolute risk aversion coefficient: Implications for generalized stochastic dominance. *Western Journal of Agricultural Economics*, 204–210.

Redl, C., Haas, R., Huber, C., & Böhm, B. (2009). Price formation in electricity forward markets and the relevance of systematic forecast errors. *Energy Economics*, *31*(3), 356–364. https://doi.org/10.1016/j.eneco.2008.12.001

Rolfo, J. (1980). Optimal hedging under price and quantity uncertainty: The case of a cocoa producer. *Journal of political economy*, *88*(1), 100–116. https://doi.org/10.1086/260849

Sakong, Y., Hayes, D. J., & Hallam, A. (1993). Hedging production risk with options. *American Journal of Agricultural Economics*, *75*(2), 408–415. https://doi.org/10.2307/1242925

Sanchez, G. A. V., Alzate, J. M., Cadena, A. I., & Benavides, J. M. (2010). Setting up standard power options to hedge price-quantity risk in a competitive electricity market: The colombian case. *IEEE Transactions on Power Systems*, *26*(3), 1493–1500.

Schwartz, E. S. (1997). The stochastic behavior of commodity prices: Implications for valuation and hedging. *the Journal of Finance*, *52*(3), 923–973.

Shapiro, A., Dentcheva, D., & Ruszczynski, A. (2021). *Lectures on stochastic programming: Modeling and theory*. SIAM.

UL Services Group. (2022). Hourly wind and solar generation profiles (1980-2021). https://www.ercot.com/files/docs/2022/12/19/ERCOT_1980-2021_WindSolarGenProfiles_FINAL_public.pdf

Vercammen, J. (1995). Hedging with commodity options when price distributions are skewed. *American Journal of Agricultural Economics*, *77*(4), 935–945. https://doi.org/10.2307/1243816

Weron, R., Bierbrauer, M., & Trück, S. (2004). Modeling electricity prices: Jump diffusion and regime switching. *Physica A: Statistical Mechanics and its Applications*, *336*(1), 39–48. https://doi.org/10.1016/j.physa.2004.01.008

Willems, B. (2005). Cournot competition, financial option markets, and efficiency.

Winzer, C., Ramírez-Molina, H., Hirth, L., & Schlecht, I. (2024). Profile contracts for electricity retail customers. *Energy Policy*, *195*, 114358.

Wolak, F. A., & Hardman, I. H. (2022). *The future of electricity retailing and how we get there* (1st ed., Vol. 41). Springer International Publishing.

Woo, C.-K., Karimov, R. I., & Horowitz, I. (2004). Managing electricity procurement cost and risk by a local distribution company. *Energy Policy*, *32*(5), 635–645.

Zhang, S., Fu, X., & Wang, X. (2012). Effects of option contracts on electricity markets: A cournot equilibrium analysis. *Asia-Pacific Power and Energy*, 1–5. https://doi.org/10.1109/appeec.2012.6307417

Zhou, D. P., Sahleh, M. A., & Tomlin, C. J. (2017). Hedging strategies for load-serving entities in wholesale electricity markets. *2017 IEEE 56th Annual Conference on Decision and Control (CDC)*.

Appendices

A Coefficients of the seasonal components of net load $S(t)$ and the residual process $S_X(t)$

Table 4: Coefficients for the seasonal components of net load and the residual process (inspired by Coulon et al. (2013), net load is shown in MW)

Hour	**Parameters for** $S(t)$							**Parameters for** $S_X(t)$				
	a_1	a_2	a_3	a_4	a_5	a_6	a_7	b_1	b_2	b_3	b_4	b_5
0	202376.95	-5785.52	-0.61	4662.38	-0.76	-86.43	4.14	-0.31	-0.15	2.12	0.29	2.34
1	162445.84	-4920.87	-0.68	4583.09	-0.76	-67.32	-46.24	-0.53	-0.08	2.02	0.20	2.26
2	116833.06	-4251.69	-0.74	4554.41	-0.76	-45.07	-207.68	-0.65	0.07	-0.52	0.12	2.16
3	68011.24	-3755.37	-0.80	4532.40	-0.76	-20.95	-464.66	-0.66	0.16	-0.35	0.10	2.24
4	16100.24	-3323.39	-0.88	4566.24	-0.75	5.08	-1050.37	-0.54	0.28	-0.48	0.13	2.53
5	24236.35	-2896.22	-1.00	4608.91	-0.76	2.00	-2413.85	-0.26	0.46	-0.57	-0.21	5.68
6	96901.72	-2392.27	5.03	4454.63	-0.81	-32.52	-4495.02	0.26	0.93	-0.49	0.19	2.67
7	77293.43	-2188.93	-1.29	4452.25	-0.78	-22.11	-4885.41	0.17	0.83	-0.53	0.19	2.69
8	262755.59	-3035.20	-0.93	4646.54	-0.76	-113.71	-3932.05	0.07	0.67	-0.58	0.22	2.59
9	528066.45	-4439.00	-0.77	4711.01	-0.77	-244.72	-3261.66	0.03	0.60	5.62	-0.26	5.72
10	624256.69	-6603.83	-0.63	5018.46	-0.78	-291.73	-2969.80	0.00	0.51	5.54	0.28	2.59
11	605929.00	-9059.86	-0.55	5236.95	-0.81	-281.93	-2810.74	0.01	-0.38	2.25	0.32	-3.63
12	545398.21	-11253.77	-0.51	5285.51	-0.86	-251.28	-2748.23	0.06	-0.26	1.90	0.31	-3.62
13	512030.39	-13002.78	-0.49	5164.70	-0.91	-234.16	-2946.51	0.24	-0.22	0.64	0.30	-3.40
14	501096.98	-14226.35	-0.48	4974.34	-0.95	-228.37	-2998.73	0.49	-0.51	-0.02	-0.29	0.06
15	504599.44	-14833.20	-0.48	4759.61	-0.97	-229.89	-2959.78	0.85	0.94	2.97	-0.34	0.24
16	438199.50	-14661.10	-0.48	4627.56	-0.94	-196.78	-2939.22	1.03	1.00	2.99	-0.35	0.08
17	286718.22	-13319.79	-0.53	4862.27	-0.81	-121.55	-2707.58	0.87	0.13	-0.38	0.22	1.82
18	191466.85	-11511.85	-0.56	5261.76	-0.81	-74.47	-2454.90	0.59	0.72	-0.58	-0.23	-0.06
19	94055.47	-10570.78	-0.56	4931.22	-0.91	-26.67	-2277.90	0.34	-0.63	2.29	-0.46	-0.26
20	148836.53	-10014.19	-0.50	4697.71	-0.93	-54.37	-2217.77	0.19	-0.63	2.07	0.44	-3.60
21	285398.54	-9292.12	-0.47	4803.80	-0.82	-123.14	-1882.68	-0.04	0.50	5.47	0.32	2.52
22	311614.80	-8071.18	-0.50	4752.58	-0.77	-137.74	-1349.12	-0.12	0.42	5.49	0.31	2.48
23	328296.86	-6669.25	-0.52	4692.68	-0.80	-147.50	-919.84	-0.21	-0.29	2.38	0.30	2.36

B Solar and wind generation model

In this appendix, we explain our renewable generation model and show some simulated solar and wind generation data.

For our renewables generation model, we use hourly generation profiles for 218 actually existing wind farms and 189 existing solar farms as provided by ERCOT (2023). The generation profiles were created using the Weather Research and Forecasting (WRF) model to simulate historical meteorological conditions. Plant-specific characteristics and observed generation data were incorporated to model operational and planned wind and solar plants. The final profiles were validated against observed generation, capturing seasonal, diurnal, and ramping behaviors. Details on the creation of the hourly generation profiles can be found in ERCOT (2022) and UL Services Group (2022). In addition to plant level data, we use hourly data on aggregate wind and solar generation from ERCOT (2024a).[8] For all these time series, we have hourly data from 2011-22.

The basic idea of our renewable generation model can be summarized as follows: First, we group the observed hourly data into *year-month-hour* groups to capture seasonal and time-of-day patterns in wind or solar generation. Next, we simulate aggregate solar and wind generation within each group based on its historical mean and variability. Then, we use the plant-specific correlation with the aggregate output to adjust each plant's individual generation around its specific historical mean. Finally, we draw random variation around that conditional mean, to randomly simulate hourly generation for each plant.

Let $G_{p,t}$ be the generation of plant p in hour t as given in the ERCOT (2023) generation profile for plant p. Each hour t belongs to a *year-month-hour* groups, which we denote by g. For example, g could represent all observations for January 2015 at 3:00 pm. Grouping the generation captures seasonal and time-of-day cycles in solar and wind generation. Let $\text{GroupMean}_{p,g}$ and $\text{GroupStd}_{p,g}$ be the mean and standard deviation of plant p in group g.

Similarly, let $G_{\text{agg},t}$ denote the observed aggregate wind (or solar) generation at time t. For each group g, we define AggMean_g and AggStd_g to be the mean and standard deviation of the observed aggregate generation. We also calculate the correlation $\rho_{p,g}$ between a plant p's observed generation $G_{p,t}$ and the observed aggregate generation $G_{\text{agg},t}$ in each group g.

For wind and solar generation respectively, we first simulate aggregate generation values $\widetilde{G}_{\text{agg},t}$ by drawing from a normal distribution centered at zero with standard deviation AggStd_g and then shifting by the group mean AggMean_g. Concretely, for each hour t in group g:

[8] We aggregate the 15-minute-level aggregate solar and wind generation to hourly generation

$$Z_{g,t} \sim \mathcal{N}(0, \text{AggStd}_g^2),$$

$$\widetilde{G}_{\text{agg},t} = Z_{g,t} + \text{AggMean}_g.$$

We set all negative simulated values to zero to ensure that simulated aggregate generation remains nonnegative.

Once the aggregate generation $\widetilde{G}_{\text{agg},t}$ is simulated, we model plant-level generation conditional on $\widetilde{G}_{\text{agg},t}$. Thereby, we capture that a wind plant's generation is typically correlated with aggregate wind generation. For each plant p in group g, we treat the correlation $\rho_{p,g}$ as the slope of a linear relationship between plant level generation $G_{p,t}$ and aggregate generation $G_{\text{agg},t}$.

$$\beta_{p,g} = \rho_{p,g} \times \frac{\text{GroupStd}_{p,g}}{\text{AggStd}_g}.$$

The coefficient $\beta_{p,g}$ measures how much plant p's generation changes with a unit change in the *aggregate* generation. Given the simulated aggregate generation $\widetilde{G}_{\text{agg},t}$, we write the conditional mean of plant p's generation as:

$$\mathbb{E}[G_{p,t} \mid \widetilde{G}_{\text{agg},t}] = \text{GroupMean}_{p,g} + \beta_{p,g}\Big(\widetilde{G}_{\text{agg},t} - \text{AggMean}_g\Big).$$

This shifts the plant's mean generation $\text{GroupMean}_{p,g}$ in response to deviations of the simulated aggregate generation from its own aggregate group mean. Here, we take into account that a wind plant's generation is typically lower if aggregate wind generation is low. Assuming a bivariate normal relationship between each plant's generation and the aggregate generation, the conditional variance of $G_{p,t}$ given $\widetilde{G}_{\text{agg},t}$ is

$$\text{Var}[G_{p,t} \mid \widetilde{G}_{\text{agg},t}] = \text{GroupStd}_{p,g}^2\Big(1 - \rho_{p,g}^2\Big).$$

Finally, we randomly draw a generation value $G_{p,t}$ for plant p conditional on the simulated aggregate generation $\widetilde{G}_{\text{agg},t}$:

$$G_{p,t}^{(\text{sim})} \sim \mathcal{N}\Big(\mathbb{E}[G_{p,t} \mid \widetilde{G}_{\text{agg},t}],\ \text{Var}[G_{p,t} \mid \widetilde{G}_{\text{agg},t}]\Big),$$

Again, we set negative generation values to zero. The result $G_{p,t}^{(\text{sim})}$ represents the simulated generation of plant p in hour t, given the simulated aggregate generation $\widetilde{G}_{\text{agg},t}$ and the historical correlation, mean, and variance patterns observed in group g.

Figure 18 shows histograms of the simulated and the observed aggregate solar and wind generation for 2019-2022. The simulated data in Graphs 18a and 18c is the histogram of the sum of the simulated hourly generation for all solar and wind plants, respectively. Graphs and 18b and 18d show the histogram of observed hourly solar and wind generation.

The graphs reveal that our solar and wind generation model creates hourly generation values that have quite similar distributions to the observed aggregate data. The only major difference is that the simulated solar and wind data shows some large outliers that are not observed in our data.

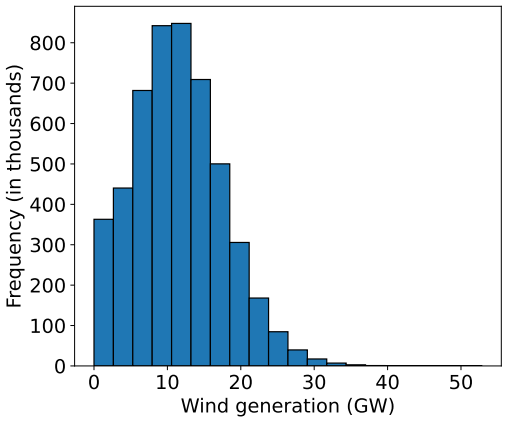

(a) Simulated wind generation (GW)

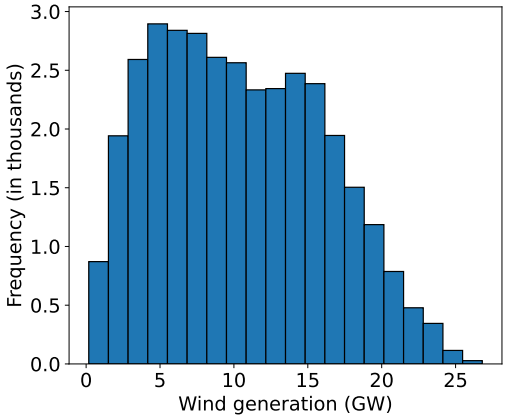

(b) Observed wind generation (GW)

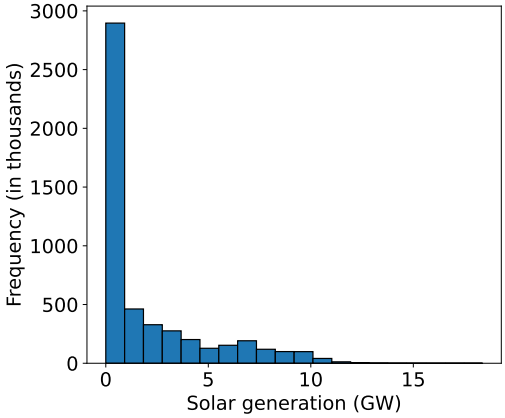

(c) Simulated solar generation (GW)

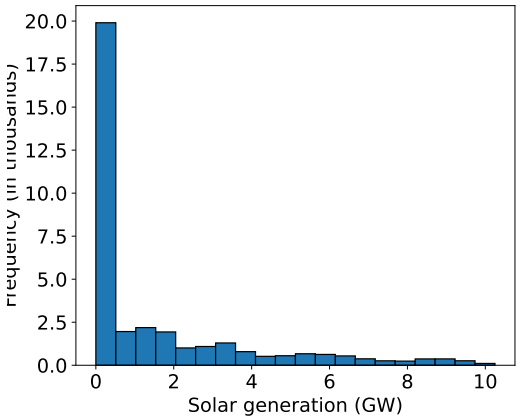

(d) Observed solar generation (GW)

Figure 18: Histogram of solar and wind generation for simulated and observed data between 2019-22

C Histogram of hourly load, net load, and gas prices for simulated and observed data between 2019-22

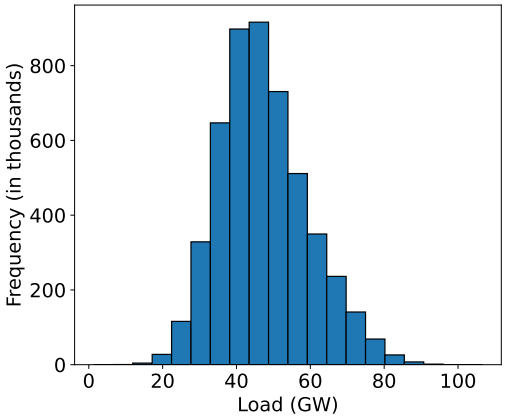

(a) Simulated load (GW)

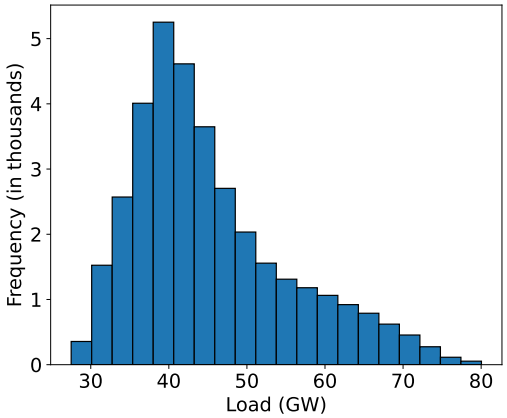

(b) Observed load (GW)

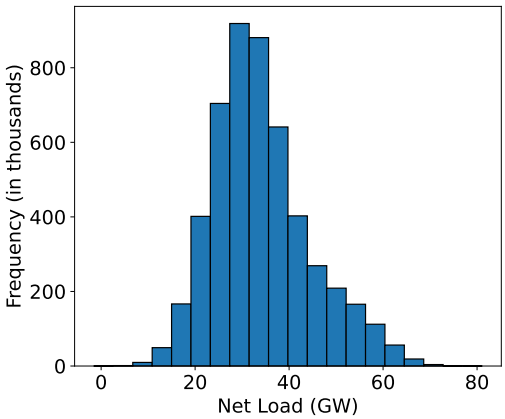

(c) Simulated net load (GW)

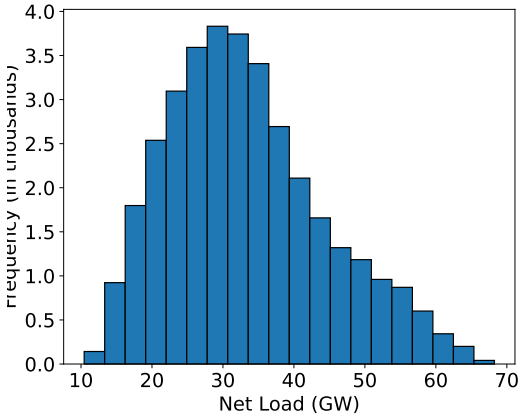

(d) Observed net load (GW)

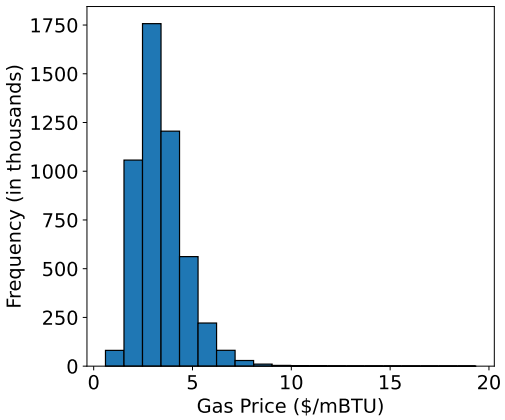

(e) Simulated gas prices ($/mBTU$)

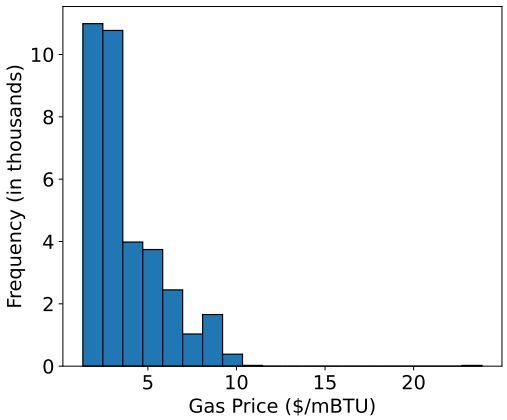

(f) Observed gas prices ($/mBTU$)

Figure 19: Histogram of hourly load, net load, and gas prices for simulated and observed data between 2019-22

In this appendix, we show histograms of simulated and observed hourly load, net load, and gas prices. In addition, we plot the relationship between load and day-ahead prices for a generator and an LSE

The left column in Figure 19 shows the simulated data and the right column shows the respective observed data. Figures 19a and 19b show that simulated and observed hourly load have similar distributions. However, observed load is more right-skewed than simulated load. This right-skewness in observed load might be driven by a positive correlation between net load and renewable generation. Our model treats net load and renewable generation as independent, which is a limitation.

Simulated and observed net load have more similar distributions as Figures 19c and 19d highlight. Yet, observed net load has a slightly higher standard deviation than load. The distribution of observed and simulated gas prices also look reasonably similar (Graphs 19e and 19f).

In Figure 20, we also plot the relationship between simulated load and day-ahead prices for an LSE and the generator. In both cases, we only find a moderate positive correlation between load and day-ahead prices.

In particular, it is surprising that very high peak prices even occur when load is below its average. On the other hand, we also sometimes observe low prices when load is really high. These plots reveal that spike prices are not mainly driven by high load, but likely by high net load in combination with random shocks like outages.

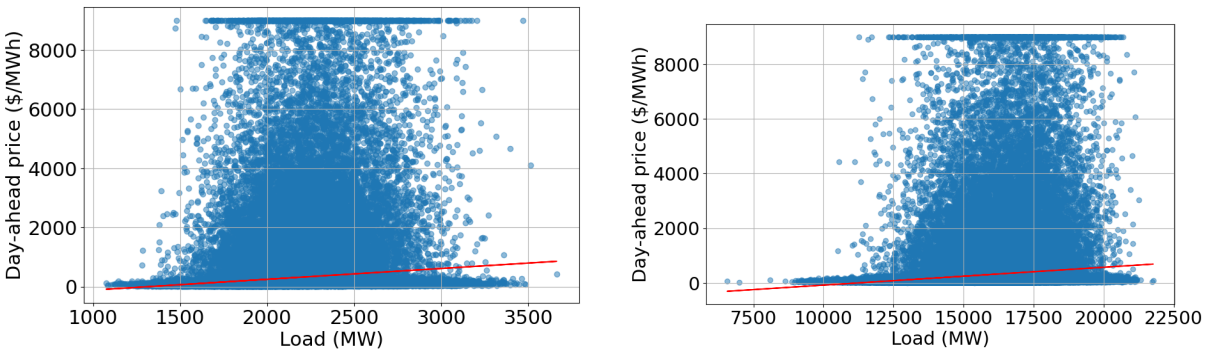

(a) LSE

(b) Generator

Figure 20: Relationship between LSE and generator's load and day-ahead electricity prices in peak delivery period 4-5 pm in August 2019

D Hedge strategies for an off-peak delivery period

In this appendix, we deep dive on off-peak delivery period Weekends 4-5 am in May 2019 which has very rare and small price spikes.

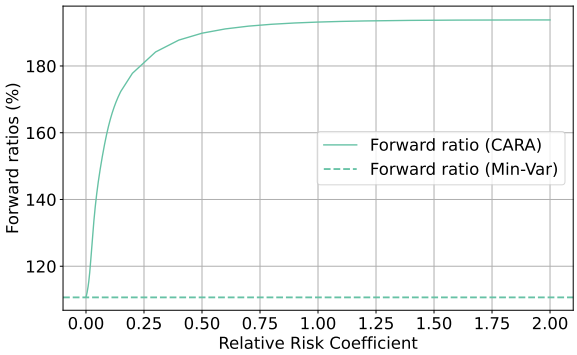

(a) LSE

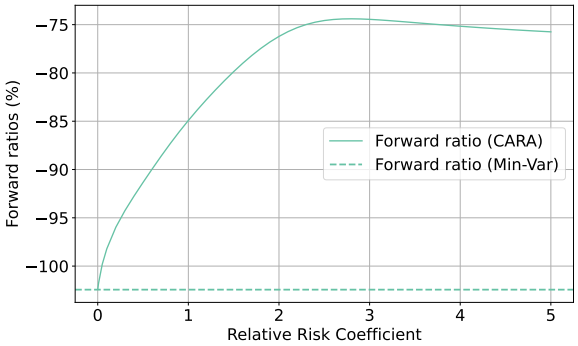

(b) Generator

Figure 21: LSE and generator's optimal forward ratio by relative risk aversion for off-peak delivery period weekends 4-5 am in May 2019

Figure 21 shows the optimal forward ratios of the LSE and the generator as a function of their risk-aversion levels for off-peak delivery period weekends 4-5 am in May 2019. The graphs reveal that the hedge strategies are very similar to the strategies in a peak period as shown in Figure 9. Interestingly, the LSE chooses higher hedge ratios in the off-peak than in the peak period. This might indicate that the LSE's load experiences larger positive outliers relative to average load in the off-peak than in the peak period. For the generator, the hedge ratios in the peak and off-peak periods are almost identical when hedging with forwards only.

Figure 22 shows how the forward ratio affects the LSE and generator's profit volatility, their conditional value at risk at the 5% level ($CVaR_{\alpha=5\%}$), and worst-case minimum profit relative to their respective mean unhedged day-ahead profit. The figure higlights that in the off-peak period, agents face the same trade-off between minimizing variance, and maximizing $CVaR_{\alpha=5\%}$ or worst-case minimum profit as discussed in section 6.1.

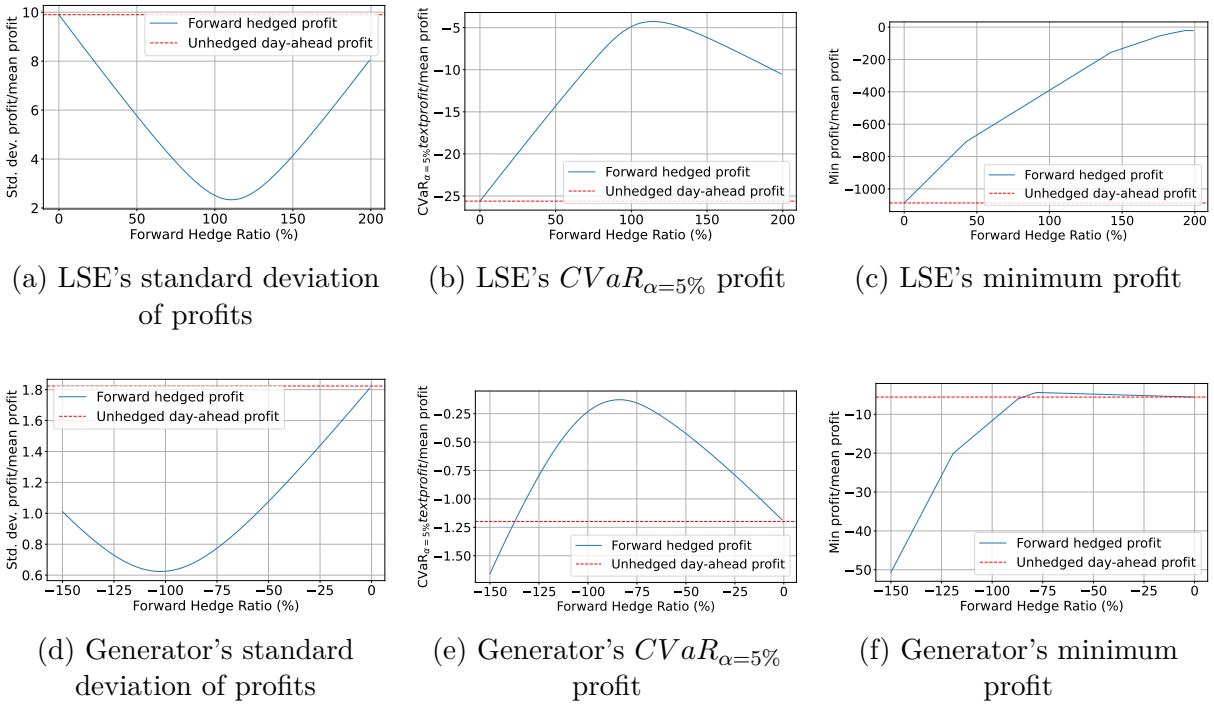

(a) LSE's standard deviation of profits

(b) LSE's $CVaR_{\alpha=5\%}$ profit

(c) LSE's minimum profit

(d) Generator's standard deviation of profits

(e) Generator's $CVaR_{\alpha=5\%}$ profit

(f) Generator's minimum profit

Figure 22: LSE and generator's profit standard deviation, ($CVaR_{\alpha=5\%}$) profit outcome, and minimum profit relative to mean unhedged day-ahead (DA) profit by forward ratio for off-peak delivery period weekends 4-5 am in May 2019

Figure 23 below shows the optimal forwards and option ratios for the combined hedge strategy as a function of agents risk aversion for the off-peak period weekends 4-5 am in May 2019. Figure 23a highlights that the LSE buys more options than forwards for moderate risk aversion in the off-peak period. When the LSE's risk aversion increases further, its option ratio rapidly declines while the forward ratio increases. Thus, the highly risk averse LSE relies far less on options in the off-peak period compared to the peak period.

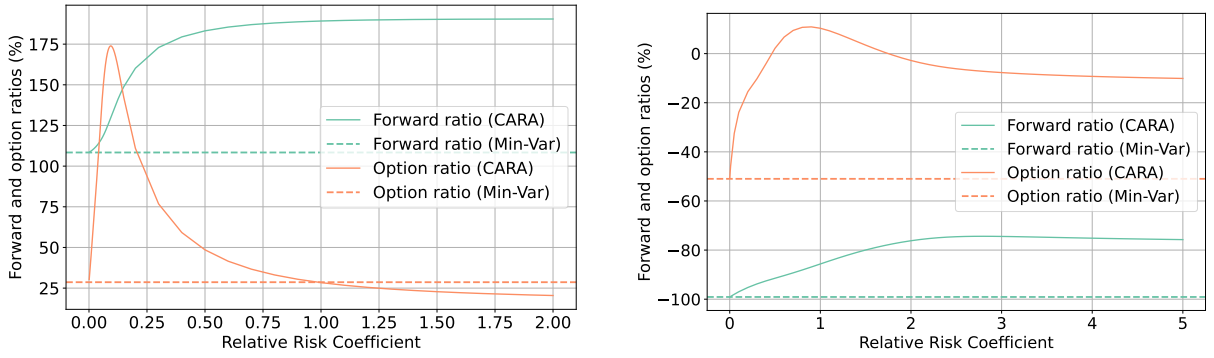

(a) LSE

(b) Generator

Figure 23: LSE and generator's optimal forward and option ratio by relative risk aversion for delivery period weekdays 4-5 pm in August 2019

Similar to the LSE, the generator also relies less on long option positions in the off-peak

period (Graph 23b). It only chooses small long option positions for moderate risk aversion levels and short positions for all other levels.

Figure 24 depicts the agents' standard deviation of profits, $CVaR_{\alpha=5\%}$ tail loss, and worst-case minimum loss as a function of the optimal forward and option ratios that are associated with a relative risk aversion level. The figure points out that the combined option and forward strategy is more successful in reducing profit variance compared to the forwards only strategy. The combined strategy also achieves substantial improvements in $CVaR_{\alpha=5\%}$, especially for the LSE. For the generator, the combined strategy trades off improvements in $CVaR_{\alpha=5\%}$ versus high worst-case losses for low-risk aversion levels. Overall, combining forwards and options hardly improves minimum worst-case losses relative to the forward-only strategy.

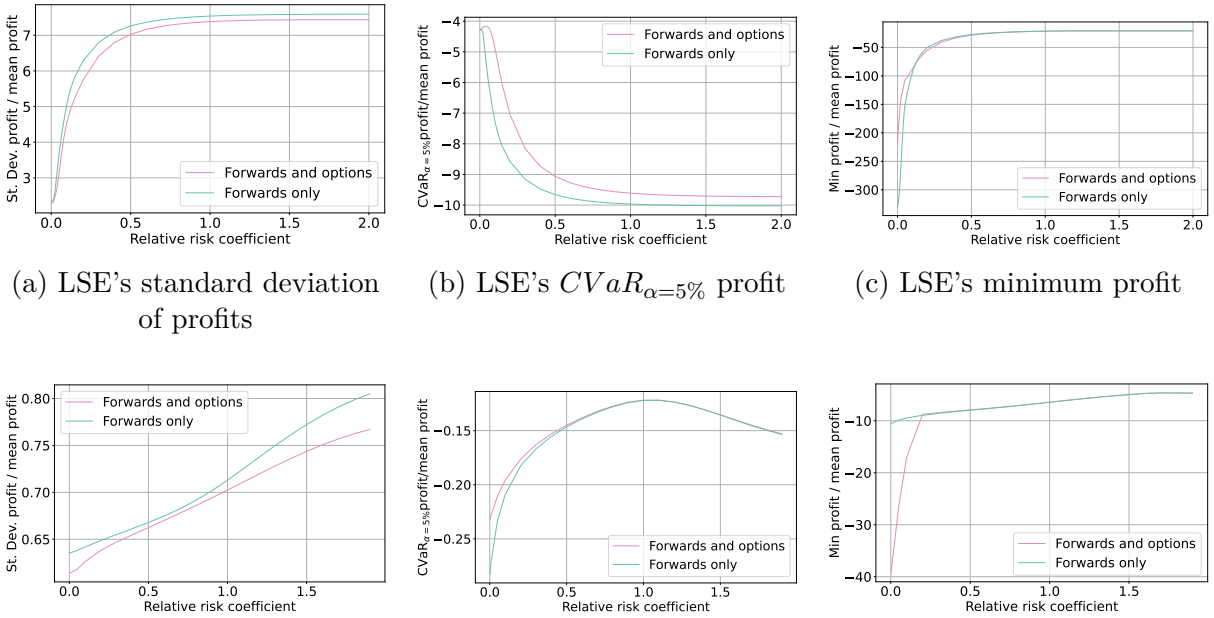

(a) LSE's standard deviation of profits

(b) LSE's $CVaR_{\alpha=5\%}$ profit

(c) LSE's minimum profit

(d) Generator's standard deviation of profits

(e) Generator's $CVaR_{\alpha=5\%}$ profit

(f) Generator's minimum profit

Figure 24: LSE and generator's profit standard deviation, minimum and maximum profit relative to mean unhedged day-ahead (DA) profit by relative risk aversion level for delivery period Weekdays 4–5 pm in August 2019

E Comparison of profit performance metrics of hedging strategies relative to the unhedged day-ahead profit

Figures 25 shows the standard deviation of profits, $CVaR_{\alpha=5\%}$ tail profit outcome, and worst-case minimum loss for the generator and LSE as a function of the optimal forward and option ratios that are associated with a relative risk aversion level. In contrast to figure 14 in section 6.2, this figure also shows the profit standard deviation, $CVaR_{\alpha=5\%}$, and worst-case minimum loss for the LSE and generator if they trade fully unhedged in the day-ahead market.

All three metrics are significantly improved when hedging with either forwards and options or with forwards only compared to the unhedged day-ahead strategy. In contrast, the added value of combining forwards and options relative to forwards only is almost negligible compared to the added value of hedging with either strategy relative to remaining unhedged.

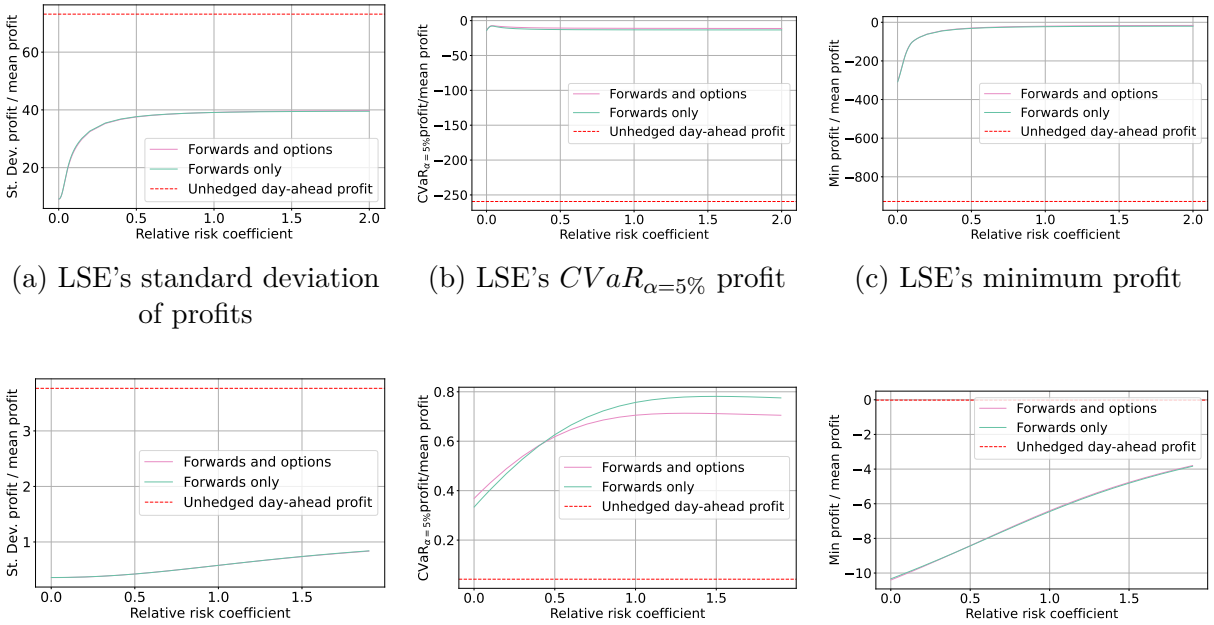

(a) LSE's standard deviation of profits

(b) LSE's $CVaR_{\alpha=5\%}$ profit

(c) LSE's minimum profit

(d) Generator's standard deviation of profits

(e) Generator's $CVaR_{\alpha=5\%}$ profit

(f) Generator's minimum profit

Figure 25: LSE and generator's profit standard deviation, minimum and maximum profit relative to mean unhedged day-ahead (DA) profit by relative risk aversion level for delivery period Weekdays 4–5 pm in August 2019